

UNIVERSITY OF OTTAWA

MCG4322

RE3 - WILDCAT ENGINEERING

Capstone Report

Volume x of y

Joey Kane - 7386330

Isaak Goldenberg - 7395188

Sawyer Woodside - 7158568

Alex Pennell - 7334789

December 8, 2017



Sponsor: Dr. Eric Lanteigne

Abstract

- i. Contents of each book (if applicable)
 - ii. Description of design
 - iii. Special considerations
 - iv. Illustration of the final design
- half page, one paragraph

Contents

| | | |
|----------|--|-----------|
| 1 | Introduction | 1 |
| 1.1 | Project Mandate | 1 |
| 1.2 | Group Problem Scope | 1 |
| 1.3 | Criteria and Restrictions | 1 |
| 1.4 | Parameterization Overview | 1 |
| 2 | Proposed Design | 5 |
| 3 | Analysis | 7 |
| 3.1 | Thruster Assembly Component Selection | 8 |
| 3.2 | Thruster Shaft | 8 |
| 3.3 | Thruster Arms | 8 |
| 3.4 | Connection To Keel | 8 |
| 3.5 | Friction Wheel Slip | 8 |
| 3.6 | Bearing Mounting (Snap-Fit) | 8 |
| 3.7 | Bolt Compression Force | 8 |
| 3.8 | Gondola Motor Shaft | 8 |
| 4 | Discussion | 9 |
| A | Instructions for Installing and Running the GUI | 15 |
| B | Code | 17 |
| B.1 | Code 1 | 17 |
| C | Additional Material | 23 |
| C.1 | Gondola Bearings | 23 |
| C.2 | Gondola Arm Deflection | 23 |
| C.3 | Gondola Arm Stresses | 24 |
| C.4 | Gondola Arm Fatigue Failure | 24 |
| C.5 | Thruster Motor | 26 |
| C.6 | Linear Actuator | 26 |
| C.7 | Thruster Arm Adhesion | 26 |
| C.8 | Thruster Bearings | 28 |
| C.9 | Vectoring Shaft Screw Axial Loading Conditions | 28 |
| C.10 | Cauchy Stress Tensor [29] | 30 |

| | |
|---|-----------|
| C.11 Previous Drag Analysis | 31 |
| C.12 New Drag Analysis | 33 |
| C.13 Thrust Force | 35 |
| D Data Sheets | 43 |
| D.1 Linear Actuator [1] | 43 |
| D.2 Bearings [18] | 44 |
| D.3 Friction Wheel Assembly | 45 |
| D.3.1 Friction Wheel [17] | 45 |
| D.3.2 Friction Wheel Set Screw [19] | 46 |
| D.3.3 Friction Wheel Motor [22] | 47 |
| D.3.4 Friction Wheel Encoder [23] | 49 |
| D.4 Spring [20] | 50 |
| D.5 Battery [7] | 51 |
| D.6 Thruster Assembly | 52 |
| D.6.1 Thruster Motor [14] | 52 |
| D.6.2 Propeller [12] | 53 |
| D.6.3 BESC [8] | 54 |
| D.6.4 Servo Motor [24] | 55 |
| D.6.5 Receiver [13] | 57 |
| D.7 Flight Control Assembly | 58 |
| D.7.1 ESC [9] | 58 |
| D.7.2 GPS Module [11] | 59 |
| D.7.3 Transceiver [15] | 60 |
| D.7.4 Flight Controller [10] | 61 |
| E Engineering Drawings | 63 |
| E.1 Parts List | 63 |
| E.2 Complete System Drawing | 63 |
| E.3 Sub-Assembly Drawings | 63 |
| E.4 Individual Part Drawings | 63 |
| F Meeting Minutes | 65 |
| F.1 Group Meeting Minutes | 65 |
| F.2 Team-Partner Meeting Minutes | 73 |
| G Recommendations for Improving the Course | 75 |

List of Figures

| | | |
|------|---|----|
| 1.1 | Overview of Modelling Paramaterization | 2 |
| 1.2 | Detailed Modelling Paramaterization | 3 |
| C.1 | Model Used to Compute the Deflection of the Gondola Arms | 23 |
| C.2 | S-N Curve for Laser Sintered Nylon [3], Used to Determine the Fatigue Failure of the Gondola Body | 25 |
| C.3 | Analysis of Carbon Fibre Adhesion (From Shigley's Machine Design [5, 484]) | 26 |
| C.4 | HS-7950TH Servo Spline Attachment [25] | 28 |
| C.5 | Drag Force Curves Computed From SolidWorks Flow Simulation | 31 |
| C.6 | Drag Force Curves Computed From SolidWorks Flow Simulation | 32 |
| C.7 | Graph of Thrust Plotted Against Airship Speed at 11000rpm With 7", 5" Pitch Diameter Propeller | 39 |
| C.8 | Test Data from Gabriel Staples Against Experimental Static Thrust Values [27] | 40 |
| C.9 | Test Data from Gabriel Staples Against Experimental Dynamic Thrust Values [27] | 41 |
| C.10 | Sample Thrust Calculation Using On-line Calculator [6] | 42 |

List of Tables

| | | |
|-----|--|----|
| 3.1 | List of All Parametrized Components | 7 |
| 3.2 | List of All Inconsequential Analysis | 7 |
| C.1 | Table of Bolt Strength for a M3-0.5 Bolt [2] | 29 |
| C.2 | Raw Data From SolidWorks Flow Simulation | 31 |
| C.3 | Airship Model Characteristics and Data [28] | 33 |
| C.4 | Drag Contribution for Various Airship Components [28] | 34 |
| C.5 | Fineness Ratios and Corresponding C_D | 35 |
| C.6 | Table of Calculated Thrust Values for Varying Airship Speeds | 38 |
| D.1 | Various Gearing For Gondola Motor Torque [22]. | 48 |

Nomenclature

| | |
|--------------|--|
| E_p | Modulus of elasticity of considered plastic hub or boss [N/mm^2] |
| F_R | Keel to assembly arm connector reaction, [N] |
| F_T | Thruster force, [N] |
| F_g | Force of gravity, [N] |
| F_{GR} | Reaction force of gondola, [N] |
| F_{K1} | Keel reaction force 1, [N] |
| F_{K2} | Keel reaction force 2, [N] |
| F_{LA} | Linear actuator force, [N] |
| F_{NB} | Normal force applied to bearing, [N] |
| F_{RSF} | Force of snap fit bearing [N] |
| F_α | Force on fastener α (hinge to gondola), [N] |
| F_β | Force on fastener β (hinge to gondola), [N] |
| F_a | Force on fastener a (hinge to gondola), [N] |
| F_{bolt} | Bolt pretension force, [N] |
| F_{brake} | Normal braking force keel reaction, [N] |
| F_b | Force on fastener b (hinge to gondola), [N] |
| F_{c1} | Connector moment couple force 1, [N] |
| F_{c2} | Connector moment couple force 2, [N] |
| F_{ffric} | Friction force acting on friction wheel, [N] |
| F_{nfric} | Normal force acting on friction wheel, [N] |
| F_{s1} | Force on friction wheel motor fastener 1 , [N] |
| F_{s2} | Force on friction wheel motor fastener 2 , [N] |
| F_{spring} | Force applied by hinge spring, [N] |
| H_{keel} | Height of the bearing arm contact point on the keel, [m] |

| | |
|-------------------|--|
| L_G | Width of gondola, [m] |
| L_a | Length from pivot point of hinge to fastener a , [m] |
| L_b | Length from pivot point of hinge to fastener b , [m] |
| L_m | Length from side of gondola to gondola drive motor hinge, [m] |
| L_s | Length from fastener to fastener of gondola motor to hinge, [m] |
| L_{SF} | Length to snap fit bearing, [m] |
| L_{ac} | Length from centerline of gondola to fastener a, [m] |
| L_{bc} | Length from centerline of gondola to fastener b, [m] |
| L_{cm} | Length from gondola wall to center of mass of gondola, [m] |
| $L_{contact}$ | Length from contact to contact of bearings on keel, [m] |
| L_{drive} | Length of gondola hinge to friction wheel contact, [m] |
| L_{hs} | Distance from the pivot of the hinge to the gondola motor fastener, [m] |
| L_{hw} | Distance from the gondola motor fastener to the contact point of the friction wheel, [m] |
| L_{rx} | Friction wheel motors shaft length, [m] |
| M_1 | Reaction moment on bearing arm, [Nm] |
| M_R | Connector moment reaction, [Nm] |
| R | Reaction force, [N] |
| $S_{compressive}$ | Compressive strength of gondola material, [Pa] |
| T_w | Friction wheel motor torque, [Nm] |
| T_{spring} | Torque of hinge spring, [Nm] |
| W_A | Weight of thruster assembly arm, [N] |
| W_E | Weight of thruster enclosure, [N] |
| W_T | Weight of thruster, [N] |
| W_c | Weight of connection piece, [N] |
| W_{LA} | Weight of linear actuator, [N] |

| | |
|-------------------|--|
| η | Safety Factor |
| μ | Coefficient of friction |
| σ' | Von Mises Stress, [Pa] |
| σ_{washer} | Compressive force of washer, [Pa] |
| σ_x | Principle stress, [Pa] |
| σ_a | Hoop stress, [N/mm ²] |
| σ_s | Allowable design stress for plastic, N/mm ² |
| $a_{airship}$ | Acceleration of airship, [m/s] |
| $a_{gondola1}$ | Acceleration of Gondola 1 , [m/s ²] |
| $a_{gondola2}$ | Acceleration of Gondola 2 , [m/s ²] |
| c | Distance from neutral axis to stress location, [m] |
| d_i | Interference diameter, [mm] |
| d_s | Hub outer diameter, [mm] |
| d_s | Shaft diameter, [mm] |
| i_a | Allowable interference, [mm] |
| $m_{airship}$ | Mass of airship, [kg] |
| $m_{gondola1}$ | Mass of Gondola 1, [kg] |
| $m_{gondola2}$ | Mass of Gondola 2, [kg] |
| r_{fw} | Radius of friction wheel, [m] |
| w_{armx} | Width of the bearing arm in the x direction, [m] |
| w_{army} | Width of the bearing arm in the y direction, [m] |

Chapter 1: Introduction

1.1 Project Mandate

The goal of the project is to overcome the current limitations involved with the control and landing of unmanned airships in adverse outdoor conditions. The airship consists of a helium filled envelope, external keel, and gondola which will act as a ballast. The moving ballast will control the pitch by the controlled displacement of the centre of mass. Propulsion will be provided by propellers in the X-Y plane of the airship. The system will have vector thrusting to allow for altitude change independent of pitch change.

1.2 Group Problem Scope

The research project led by Dr. Eric Lanteigne involves designing a system to allow for the control of an unmanned airship. The goal of the project is to create a system that controls the airship by changing the position of the centre of mass to initiate pitch change. This pitch change, along with forward propulsion, will drive the airship in a given direction. The design team will be responsible for creating a system, where a gondola that acts as a ballast, will move along a nonlinear, diamond-shaped keel in order to initiate pitch change of an airship. Ideally, the system will be able to incur a pitch change of up to ninety degrees, allowing the airship to descend straight downwards. Currently, all designs must be scalable as specifications of the airship envelope have yet to be finalized. The unmanned airship must be capable of flying outdoors and be able to carry a payload of between 0.2kg and 0.5kg. The main components of the design can be split up into: Gondola Design, Gondola Movement, Securing Gondola to Keel, Gondola Position Measurement, Securing the Propellers, Thrust Vectoring, Batteries, and Wire Management.

1.3 Criteria and Restrictions

The propellers will be in the X-Y plane, in line with the centre of volume. This eliminates any moments from the propellers that lead to imbalance and unwanted pitch variations. The gondola will be able to move along the varying curvature of the keel using a hinged-gondola. The driving mechanism will be two friction wheels with the additional support of 4 driven bearings. The cross-section of the keel is diamond-shaped, however it is not torsionally constant, therefore the vertexes are not coincident on the curved section. Once the airship has been constructed, a Special Flight Operations Certificate (SFOC) issued by Transport Canada will be necessary in order to fly the airship lawfully.

1.4 Parameterization Overview

A high level overview of the system's parameterization is shown in Figure 1.1.

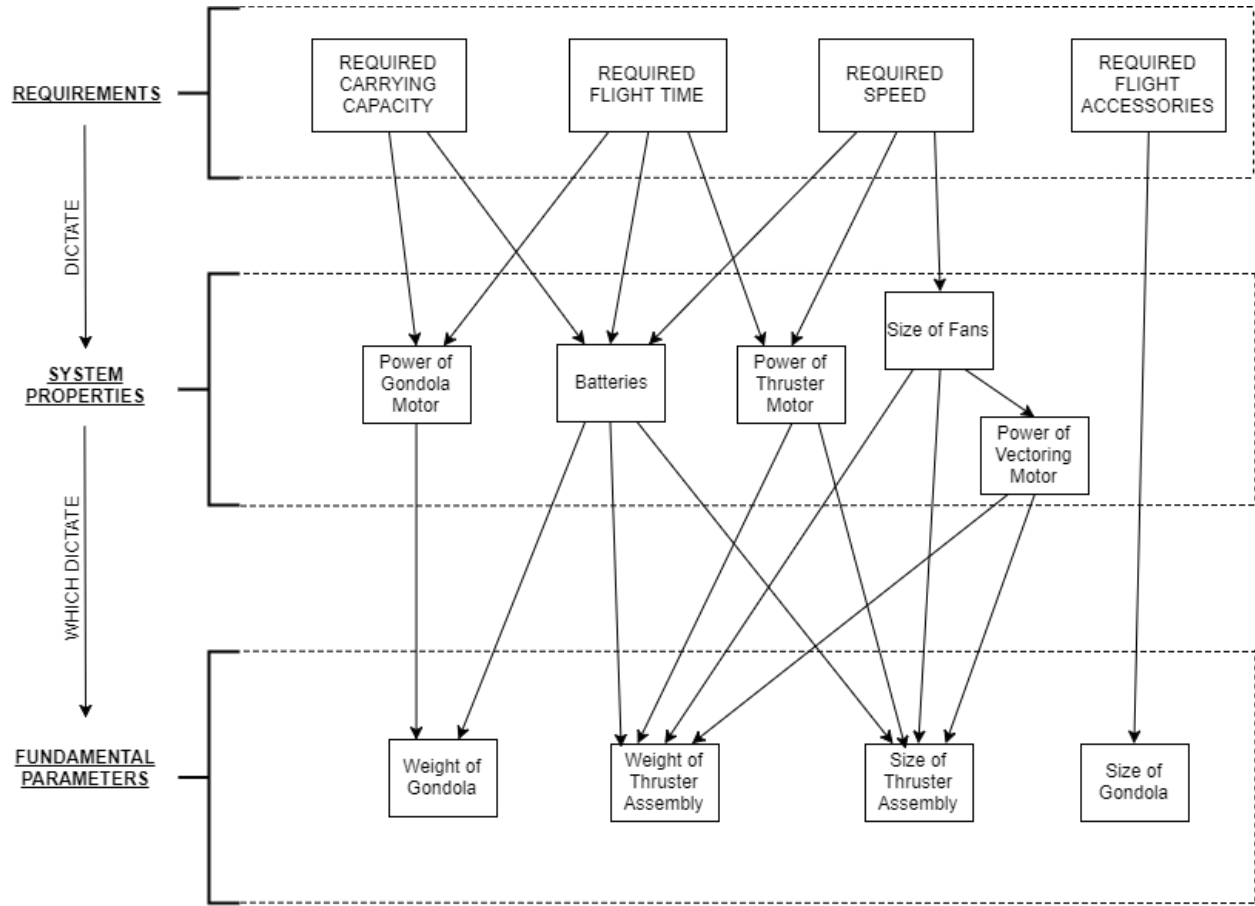


Figure 1.1: Overview of Modelling Parameterization

Figure 1.2 is a more detailed parameterization outline, which shows how user inputs will be converted to forces using an iterative approach. This approach will be used to compute all forces shown in Section ADD HERE.

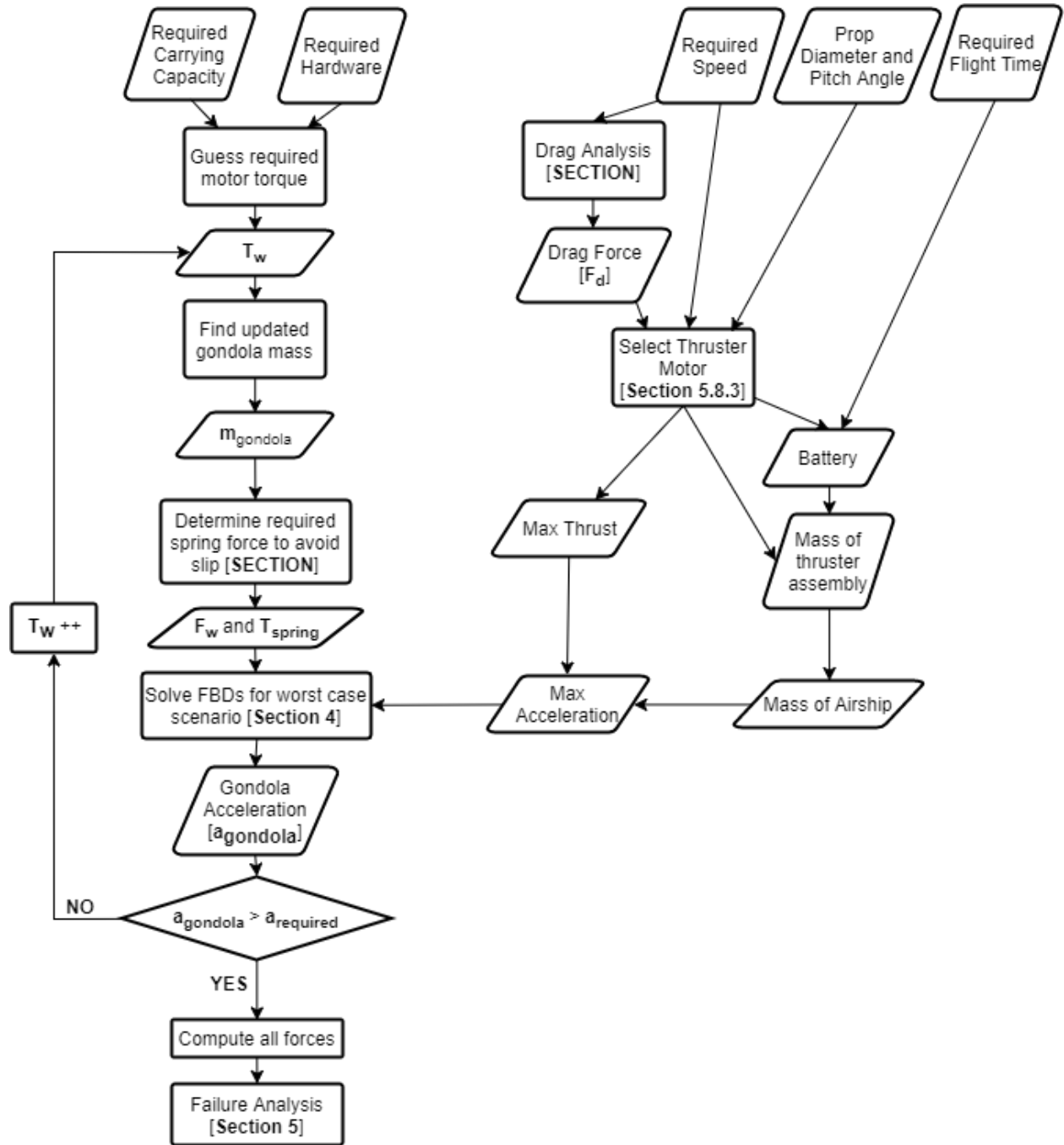


Figure 1.2: Detailed Modelling Parameterization

Once all of the forces acting on the body are computed, failure analyses for each part are conducted in Section ADD HERE.

Chapter 2: Proposed Design

Text

make a change

triangles are strong

Chapter 3: Analysis

Table 3.1: List of All Parametrized Components

| Section | Analysis | Parametrized Part | Failure Likelihood |
|---------|---------------------------------------|----------------------------|--------------------|
| 3.1 | Thruster Assembly Component Selection | Thruster Battery | MEDIUM |
| | | Propeller Diameter | |
| | | Motor | |
| | | Thruster Shaft Length | |
| | | Diameter of Encasement | |
| 3.2 | Thruster Shaft | Diameter of Thruster Shaft | MEDIUM |
| | | Thread Type | |
| | | Material Type | |
| | | Bearing Dimensions | |
| 3.3 | Thruster Arms | Width | HIGH |
| 3.4 | Connection To Keel | Thickness | HIGH |
| 3.5 | Friction Wheel Slip | Width of Insert | MEDIUM |
| | | Spring Force | |
| 3.7 | Gondola Hinge Bolts | Motor Torque | MEDIUM |
| 3.6 | Gondola Bearing Snap-Fit | Diameter of Washers | HIGH |
| | | Depth of Cut | |
| | | Distance of Arms from Keel | |

Table 3.2: List of All Inconsequential Analysis

| Section | Inconsequential Analysis | Failure Likelihood |
|---------|-------------------------------------|--------------------|
| C.1 | Gondola Bearings | LOW |
| C.2 | Gondola Arm Deflection | LOW |
| C.4 | Gondola Arm Fatigue | LOW |
| C.3 | Gondola Arm Stresses | LOW |
| C.5 | Thruster Motor | LOW |
| C.6 | Linear Actuator | LOW |
| C.8 | Thruster Bearings | LOW |
| C.7 | Thruster and Arm Adhesion | LOW |
| C.9 | Vectoring Motor Shaft Axial Loading | LOW |

3.1 Thruster Assembly Component Selection

3.2 Thruster Shaft

3.3 Thruster Arms

3.4 Connection To Keel

3.5 Friction Wheel Slip

3.6 Bearing Mounting (Snap-Fit)

3.7 Bolt Compression Force

3.8 Gondola Motor Shaft

Chapter 4: Discussion

Discussion and Critical Review of Design aka Talk shit about ourselves

Bibliography

- [1] Actuonix Motion Devices. Miniature Linear Motion Series - L12, 2016. URL <https://s3.amazonaws.com/actuonix/Actuonix+L12+Datasheet.pdf>.
- [2] Advanced Mechanical Engineering Solutions. Metric Bolt Grades Strength, 2017. URL <http://www.amesweb.info/Screws/Metric\Bolt\Grades\Strength.aspx>.
- [3] Hoda Amel. *Investigating the Cyclic Performance of Laser Sintered Nylon 12*. PhD thesis, University of Sheffield, 2015. URL <http://etheses.whiterose.ac.uk/11927/1/Investigating the Cyclic Performance of Laser Sintered Nylon 12-Hoda Amel-110203386.pdf>.
- [4] Steven A. Brandt and American Institute of Aeronautics and Astronautics. *Introduction to aerodynamics : a design perspective*. American Institute of Aeronautics and Astronautics, 2004. ISBN 9781563477010.
- [5] Budynas and Nisbett. Shigley's Mechanical Engineering Design, Eighth Edition. *Analysis*, page 1059, 2006. ISSN 0717-6163. doi: 10.1007/s13398-014-0173-7.2.
- [6] Szabolcs Füzesi. Static Thrust Calculator - STRC, 2017. URL <http://www.godolloairport.hu/calc/strc\eng/index.htm>.
- [7] HobbyKing. Rhino 2250mAh 3S 11.1v 40C Lipoly Pack, . URL https://hobbyking.com/en\us\rhino-2250mah-3s-11-1v-40c-lipoly-pack.html?{_\}\{_\}\{_\}store=en\us.
- [8] HobbyKing. TURNIGY Plush 10amp Speed Controller w/BEC, . URL <https://hobbyking.com/en\us/turnigy-plush-10amp-9gram-speed-controller.html>.
- [9] HobbyKing. Turnigy 20A BRUSHED ESC, . URL https://hobbyking.com/en\us/turnigy-20a-brushed-esc.html?{_\}\{_\}\{_\}store=en\us.
- [10] HobbyKing. PixFalcon Micro PX4 Autopilot, . URL <https://hobbyking.com/en\us/pixfalcon-micro-px4-autopilot.html>.
- [11] HobbyKing. UBLOX Micro M8N GPS Compass Module (1pc), . URL <https://hobbyking.com/en\us\ublox-micro-m8n-gps-compass-module-1pc.html>.
- [12] HobbyKing. Aerostar Carbon Fibre Propeller 7x5, . URL https://hobbyking.com/en\us\aedostar-carbon-fibre-propeller-7x5-1pcs.html?{_\}\{_\}\{_\}store=en\us.
- [13] HobbyKing. FrSky TFR6M 2.4Ghz 6CH Micro Receiver FASST Compatible, . URL <https://hobbyking.com/en\us/frsky-tfr6m-2-4ghz-6ch-micro-receiver-fasst-compatible.html>.

- [14] HobbyKing. HobbyKing® TM 2612 Brushless Outrunner 1900KV, . URL https://hobbyking.com/en{_}us/hobbykingr-tm-2612-brushless-outrunner-1900kv.html?gclid=CjwKCAjwgvf0BRB7EiwAeP7ehmx-1gQwKEcajtpPc1NNf0p82N1T2DdM6I-PFOINiIxTERGAn2ZBdhoCJIQQAvD{_}BwE{_}gclsrc=aw.ds.
- [15] HobbyKing. Micro HKPilot Telemetry radio Set With Integrated PCB Antenna 915Mhz, . URL https://hobbyking.com/en{_}us/micro-hkpilot-telemetry-radio-set-with-integrated-pcb-antenna-915mhz.html.
- [16] MatWeb. Overview of materials for Epoxy/Carbon Fiber Composite, 2017. URL http://www.matweb.com/search/DataSheet.aspx?MatGUID=39e40851fc164b6c9bda29d798bf3726{_}ckck=1.
- [17] McMaster-Carr. McMaster-Carr - Neoprene Roller, Drive, Aluminum Hub, 5/8" Roller Diameter, 3/16" Roller Width, . URL <https://www.mcmaster.com/{#}60885k31/=19r8ni4>.
- [18] McMaster-Carr. McMaster-Carr - General Purpose Plastic Ball Bearing, with Stainless Steel Ball, for 1/4" Shaft Diameter, 5/8" OD, . URL <https://www.mcmaster.com/{#}6455k2/=19n14h4>.
- [19] McMaster-Carr. McMaster-Carr - Alloy Steel Cup-Point Set Screw, Black Oxide, 8-32 Thread, 1/4" Long, . URL <https://www.mcmaster.com/{#}91375a190/=19r8q0o>.
- [20] McMaster-Carr. Music-Wire Steel Torsion Sring, . URL <https://www.mcmaster.com/{#}9271k641/=19n18gv>.
- [21] Michigan Technological University. Properties of Seleced Matrices, 2017. URL <http://www.mse.mtu.edu/{-}drjohn/my4150/props.html>.
- [22] Pololu. 50:1 Micro Metal Gearmotor HP 6V, . URL <https://www.pololu.com/product/998/specs>.
- [23] Pololu. Magnetic Encoder Pair Kit for Micro Metal Gearmotors, 12 CPR, 2.7-18V (HPCB compatible), . URL <https://www.pololu.com/product/3081/pictures>.
- [24] RobotShop. HS-7950TH Ultra Torque HV Coreless Titanium Gear Servo - RobotShop. URL http://www.robotshop.com/ca/en/hs-7950th-ultra-torque-coreless-titanium-gear-servo.html?gclid=CjwKCAjwgvf0BRB7EiwAeP7ehmVw7Ku4Ih2HYJeFV34wtpf0lmQIOCX5BXYQ00f48oI4lG0zHuABnRoCKiEQAvD{_}BwE.
- [25] Servo City. HS-7950TH Servo, 2017. URL <https://www.servocity.com/hs-7950th-servo>.
- [26] Gabriel Staples. Propeller Static & Dynamic Thrust Calculation - Part 1 of 2, 2013. URL <http://www.electricrcaircraftguy.com/2013/09/propeller-static-dynamic-thrust-equation.html>.

- [27] Gabriel Staples. Propeller Static & Dynamic Thrust Calculation - Part 2 of 2, 2015.
URL <http://www.electricrcaircraftguy.com/2014/04/propeller-static-dynamic-thrust-equation-background.html>.
- [28] War Department. Technical Manual of Airship Aerodynamics. Technical report, Washington, 1941. URL https://www.faa.gov/regulations__policies/handbooks__manuals/aviation/media/airship__aerodynamics.pdf.
- [29] Wikipedia. Cauchy Stress Tensor, 2017. URL https://en.wikipedia.org/wiki/Cauchy__stress__tensor.

Appendix A: Instructions for Installing and Running the GUI

yep

Appendix B: Code

B.1 Code 1

```
1 function lab1
2
3 disp('_____');
4 disp('_____');
5 disp('| Lab 1 |');
6 disp('_____');
7 disp('_____');
8
9
10 % Point we are using as x_i
11 x = 5.0;
12
13 % Delta x's that we will use in our finite-difference approximations
14 dx1 = 0.5;
15 dx2 = dx1/2;
16 dx3 = dx2/2;
17 dx4 = dx3/2;
18 dx5 = dx4/2;
19
20 % Exact derivative of y at x=5
21 exact1 = dy(5.0);
22
23 %%%%%%
24 % Approximation of the first derivative
25
26 approx11 = dyapprox(x, dx1);
27 approx12 = dyapprox(x, dx2);
28 approx13 = dyapprox(x, dx3);
29 approx14 = dyapprox(x, dx4);
30 approx15 = dyapprox(x, dx5);
31
32 % Errors using first-order method
33 disp('Errors for first-order finite-difference , (first column of table)')
34 error11 = abs(exact1 - approx11)
35 error12 = abs(exact1 - approx12)
36 error13 = abs(exact1 - approx13)
37 error14 = abs(exact1 - approx14)
38 error15 = abs(exact1 - approx15)
```

```

40 % Order of convergence
41 disp('Actual order of convergence for first-order method, (second column of table)')
42 order11 = log(error12/error11)/log(dx2/dx1)
43 order12 = log(error13/error12)/log(dx3/dx2)
44 order13 = log(error14/error13)/log(dx4/dx3)
45 order14 = log(error15/error14)/log(dx5/dx4)
46
47%%%%%%%%%%%%%
48 % Approximation of the second derivative
49
50 %Exact second derivative of y at x=5
51 exact2 = d2y(5.0);
52
53 approx21 = d2yapprox(x, dx1);
54 approx22 = d2yapprox(x, dx2);
55 approx23 = d2yapprox(x, dx3);
56 approx24 = d2yapprox(x, dx4);
57 approx25 = d2yapprox(x, dx5);
58
59 % Errors using first-order method
60 disp('Errors for first-order finite-difference, (first column of table)')
61 error21 = abs(exact2 -approx21)
62 error22 = abs(exact2 -approx22)
63 error23 = abs(exact2 -approx23)
64 error24 = abs(exact2 -approx24)
65 error25 = abs(exact2 -approx25)
66
67 % Order of convergence
68 disp('Actual order of convergence for first-order method, (second column of table)')
69 order21 = log(error22/error21)/log(dx2/dx1)
70 order22 = log(error23/error22)/log(dx3/dx2)
71 order23 = log(error24/error23)/log(dx4/dx3)
72 order24 = log(error25/error24)/log(dx5/dx4)
73
74%%%%%%%%%%%%%
75 % Approximation of the third derivative
76
77 %Exact third derivative of y at x=5
78 exact3 = d3y(5.0);
79
80 approx31 = d3yapprox(x, dx1);
81 approx32 = d3yapprox(x, dx2);
82 approx33 = d3yapprox(x, dx3);
83 approx34 = d3yapprox(x, dx4);
84 approx35 = d3yapprox(x, dx5);

```

```

85
86 % Errors using first-order method
87 disp('Errors for first-order finite-difference, (first column of table)')
88 error31 = abs(exact3 -approx31)
89 error32 = abs(exact3 -approx32)
90 error33 = abs(exact3 -approx33)
91 error34 = abs(exact3 -approx34)
92 error35 = abs(exact3 -approx35)
93
94 % Order of convergence
95 disp('Actual order of convergence for first-order method, (second column of table)')
96 order31 = log(error32/error31)/log(dx2/dx1)
97 order32 = log(error33/error32)/log(dx3/dx2)
98 order33 = log(error34/error33)/log(dx4/dx3)
99 order34 = log(error35/error34)/log(dx5/dx4)
100
101%%%%%%%%%%%%%
102%%%%%%%%%%%%%
103% Produce plots
104%%%%%%%%%%%%%
105%%%%%%%%%%%%%
106
107% Number of points in the plots
108% - Adjust this to adjust how small Delta x gets.
109% It starts at 1/2 and is divided by 2 "n" times
110 n = 33;
111
112% Initialize Storage
113 dxs = zeros(n,1);
114 errors1 = zeros(n,1);
115 errors2 = zeros(n,1);
116 errors3 = zeros(n,1);
117
118% loop through, filling "d_xs", "errors1", "errors2", and "errors3".
119 for i = 1:n
120 % Each time through the loop, Delta x is half as big
121 d_xs(i) = 0.5^i;
122 errors1(i)=abs(exact1-dyapprox(x,d_xs(i)));
123 errors2(i)=abs(exact2-d2yapprox(x,d_xs(i)));
124 errors3(i)=abs(exact3-d3yapprox(x,d_xs(i)));
125 end
126
127% Compute the log of the inverse of delta x
128 loginvdxs = log10(1./d_xs);
129

```

```

130 % Compute the log of the errors
131 logerrors1 = log10(errors1);
132 logerrors2 = log10(errors2);
133 logerrors3 = log10(errors3);

134

135 % Compute reference lines with the expected slope
136 %   - the "-2" is just an offset so that the reference
137 %     line does not intersect the error line.
138 reffline1 = -3*loginvdxs -2;
139 reffline2 = -2*loginvdxs -2;
140 reffline3 = -1*loginvdxs -2;

141

142 %%%%%%
143 % Make three figures
144 figure(1);
145 plot(loginvdxs,logerrors1,'-o',loginvdxs,reffline1)
146 legend('finite-difference','reference', 'slope = -3')
147 title('Third-order finite-difference error for the first derivative as a function of Delta x')
148 xlabel('log10(1/Delta x)')
149 ylabel('log10(error)')

150

151 figure(2);
152 plot(loginvdxs,logerrors2,'-o',loginvdxs,reffline2)
153 legend('finite-difference','reference', 'slope = -2')
154 title('Second-order finite-difference error for the second derivative as a function of Delta x')
155 xlabel('log10(1/Delta x)')
156 ylabel('log10(error)')

157

158 figure(3);
159 plot(loginvdxs,logerrors3,'-o',loginvdxs,reffline3)
160 legend('finite-difference','reference', 'slope = -1')
161 title('First-order finite-difference error for the third derivative as a function of Delta x')
162 xlabel('log10(1/Delta x)')
163 ylabel('log10(error)')

164

165 end

166

167

168 %%%%%%
169 % The function we are analysing evaluated at x
170 %%%%%%
171 function output = y(x)

```

```

172     output = (x^3)*sin(x);
173 end
174
175 %%%%%%%%%%%%%%%%%%%%%%%%%%%%%%%%%%%%%%
176 % The exact derivative of the function we are analysing
177 % evaluated at x.
178 %%%%%%%%%%%%%%%%%%%%%%%%%%%%%%%%%%%%%%
179 function output = dy(x)
180     output = 3*x^2*sin(x)+x^3*cos(x);
181 end
182
183 %%%%%%%%%%%%%%%%%%%%%%%%%%%%%%%%%%%%%%
184 % The exact second derivative of the function we are analysing
185 % evaluated at x.
186 %%%%%%%%%%%%%%%%%%%%%%%%%%%%%%%%%%%%%%
187 function output = d2y(x)
188     output = 6*x^2*cos(x)+(6*x-x^3)*sin(x);
189 end
190
191 %%%%%%%%%%%%%%%%%%%%%%%%%%%%%%%%%%%%%%
192 % The exact third derivative of the function we are analysing
193 % evaluated at x.
194 %%%%%%%%%%%%%%%%%%%%%%%%%%%%%%%%%%%%%%
195 function output = d3y(x)
196     output = (18*x-x^3)*cos(x)+(6-9*x^2)*sin(x);
197 end
198
199 %%%%%%%%%%%%%%%%%%%%%%%%%%%%%%%%%%%%%%
200 % A third-order approximation to the derivative of y
201 % at x using a step size of "dx"
202 %%%%%%%%%%%%%%%%%%%%%%%%%%%%%%%%%%%%%%
203 function output = dyapprox(x,dx)
204     output = (1.0/(6*dx))*(-11*y(x)+18*y(x+dx)-9*y(x+2*dx)+2*y(x+3*dx));
205 end
206
207 %%%%%%%%%%%%%%%%%%%%%%%%%%%%%%%%%%%%%%
208 % A second-order approximation to the second derivative of y
209 % at x using a step size of "dx"
210 %%%%%%%%%%%%%%%%%%%%%%%%%%%%%%%%%%%%%%
211 function output = d2yapprox(x,dx)
212     output = 1.0/(dx*dx)*(2*y(x)-5*y(x+dx)+4*y(x+2*dx)-y(x+3*dx));
213 end
214
215 %%%%%%%%%%%%%%%%%%%%%%%%%%%%%%%%%%%%%%
216 % A first-order approximation to the third derivative of y

```

```
217 % at x using a step size of "dx"
218 %%%%%%%%%%%%%%%%%%%%%%%%%%%%%%%%%%%%%%
219 function output = d3yapprox(x,dx)
220     output = 1.0/(dx*dx*dx)*(-1*y(x)+3*y(x+dx)-3*y(x+2*dx)+y(x+3*dx));
221 end
```

Appendix C: Additional Material

C.1 Gondola Bearings

Test

C.2 Gondola Arm Deflection

To ensure that the gondola will not fall off of the keel during operation, a deflection calculation is computed on the gondola arm. The maximum deflection of the gondola arm is modelled as shown below:

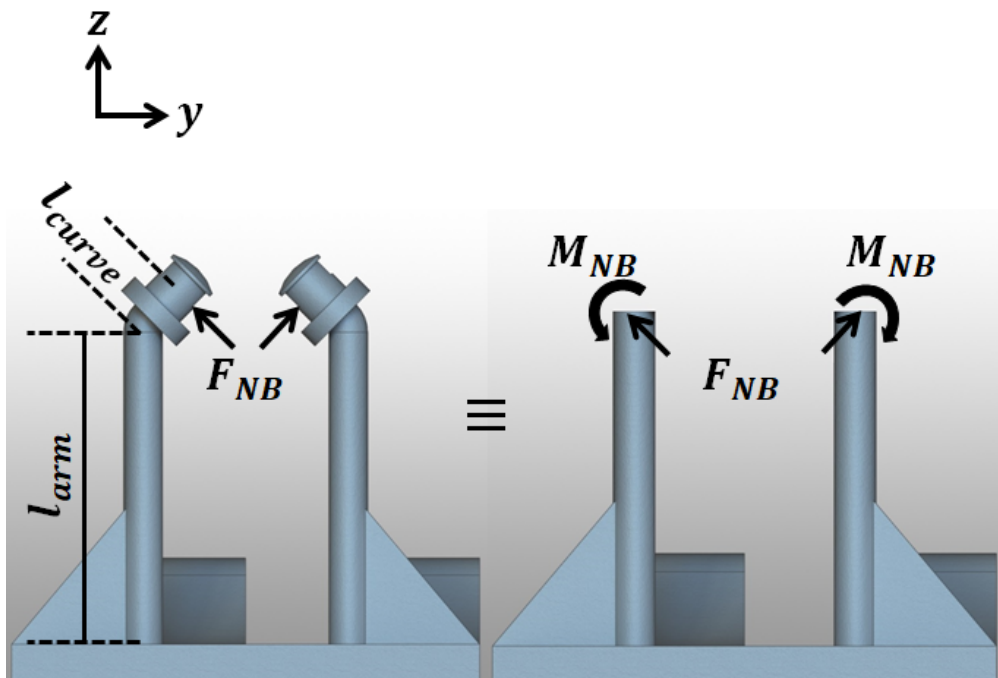


Figure C.1: Model Used to Compute the Deflection of the Gondola Arms

For the sake of simplicity, the curved section at the very top is ignored and the force is translated from the curved section to the straight section using a force-moment couple. The moment M_{NB} is computed as $M_{NB} = F_{NB}l_{curve}$. Furthermore, the rib seen in Figure C.1 is ignored. The deflection criteria will be computed without the rib, and the rib will be added as an extra preventative measure, to ensure the member is rigid enough.

The deflection will be calculated using simple beam equations. The force F_{NB} is resolved into *y* and *z* components. The deflection is then computed in three separate parts, as shown below:

$$\delta_{GondolaArm} = \delta_{axial} + \delta_{bendingforce} + \delta_{bendingmoment} \quad (C.1)$$

$$\delta_{GondolaArm} = \left(\frac{F_{NB_z} l_{arm}}{AE} \right) \hat{k} + \left(\frac{F_{NB_y} l_{arm}^3}{3EI} + \frac{M_{NB} l_{arm}^2}{2EI} \right) \hat{j} \quad (C.2)$$

The failure possibility here would be for the arm to deflect enough that the gondola falls off the keel. This occurs when the total deflection δ is larger than $0.5cm$, which is half of the width of the keel face. Since both arms can deflect at the same time, they can be combined to reach $0.5cm$. Therefore it is required that the result of Equation C.2 be less than $0.25cm$. Therefore the equation to optimize is:

$$0.25 \leq \sqrt{\left(\frac{F_{NB_z} l_{arm}}{AE} \right)^2 + \left(\frac{F_{NB_y} l_{arm}^3}{3EI} + \frac{M_{NB} l_{arm}^2}{2EI} \right)^2} \quad (C.3)$$

C.3 Gondola Arm Stresses

The failure of the gondola arm will be analysed in a very similar fashion to the gondola arm deflection. Once again, Figure C.1 is used as the basis for the analysis. Instead of deflection however, stress at the inner corner of the arm is found as:

$$\sigma_{GondolaArm} = \sigma_{axial} + \sigma_{bendingforce} + \sigma_{bendingmoment} \quad (C.4)$$

$$\sigma_{GondolaArm} = \left(\frac{F_{NB_z}}{A} \right) \hat{k} + \left(\frac{F_{NB_y} l_{arm} c}{I} + \frac{M_{NB} c}{I} \right) \hat{j} \quad (C.5)$$

These stresses are converted to principle stresses (as shown in Appendix C.10). These principle stresses are then used to determine the safety factor by Brittle Mohr-Coulomb Theory [5, 227].

Since $\sigma_a > \sigma_b > 0$,

$$\eta = \frac{S_{ut}}{\sigma_a} \Rightarrow 1.5 \geq \frac{S_{ut}}{\sigma_a} \quad (C.6)$$

C.4 Gondola Arm Fatigue Failure

The loading and unloading of the plastic gondola arm due to the reaction force of the keel on the gondola motor could potentially cause a fatigue failure. A paper on cyclic performance of Laser Sintered Nylon [3] was used to quantify the effects of fatigue on the plastic. Very little research has been done for fatigue failure of 3D printed material. The laser sintering process is similar to 3D printing in that it melts layers of plastic in succession to obtain complex geometries with no pre-existing tooling required. Because of this, the laser sintering process creates shear planes, much like those created in 3D printing. For this reason, the paper was as a basis for the fatigue analysis of the 3D printed part, as these shear planes are

critical to the fatigue strength of the material.

The S-N curve shown in Figure C.2 was used to determine the maximum nominal stress that the gondola could take, thus defining the criteria for failure.

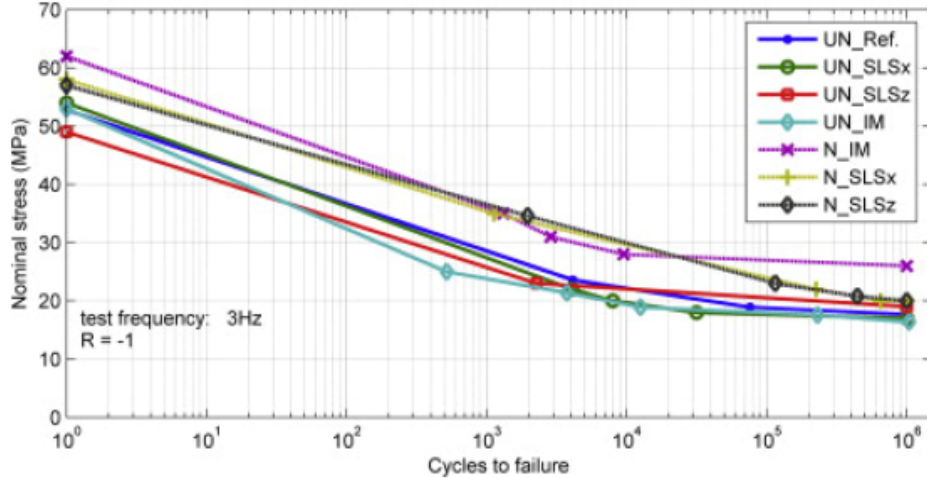


Figure C.2: S-N Curve for Laser Sintered Nylon [3], Used to Determine the Fatigue Failure of the Gondola Body

Assuming that the loading frequency is not higher than around 3hz, no appreciable heat is generated and thus the loading frequency should not affect the cycles to failure. Assuming SLS nylon, the maximum nominal stress for infinite life (10^6 cycles) is 17 MPa . Any higher and the part will fail after enough loading cycles.

To find the nominal stress, the amount of stress fluctuation which the gondola arm will sustain needs to be computed. For this, the lowest stress will be when the gondola is not moving, and is only loaded by the weight of the gondola itself. The highest stress will be when the gondola motor is on at full force, at the worst case scenario **DESCRIBED HERE** bending the gondola arm. These both conditions are computed using **ISAAKS SHIT HERE**, and two values of F_{NB} are found. The difference between the two is the fluctuation of stress.

$$\sigma_{worst} = \underbrace{\left[\left(\frac{F_{NB_z}}{A} \right) \hat{k} + \left(\frac{F_{NB_y} l_{arm} c}{I} + \frac{M_{NB} c}{I} \right) \hat{j} \right]}_{\text{Worst Case } F_{NB}}, \quad \sigma_{best} = \underbrace{\left[\left(\frac{F_{NB_z}}{A} \right) \hat{k} + \left(\frac{F_{NB_y} l_{arm} c}{I} + \frac{M_{NB} c}{I} \right) \hat{j} \right]}_{\text{Best Case } F_{NB}} \quad (\text{C.7})$$

The principle stress for each case σ_a is found, and the difference is computed to get the nominal strength, which must be less than 17 MPa . Therefore the optimized equation is:

$$17Mpa \geq |\sigma_{a_{best}} - \sigma_{a_{worst}}| \quad (\text{C.8})$$

C.5 Thruster Motor

C.6 Linear Actuator

C.7 Thruster Arm Adhesion

To connect the carbon fibre arm to the aluminium body which holds the thruster assembly, epoxy will be used. The carbon fibre arm will slide into an aluminium pocket welded to the aluminium thruster plate, as shown in Figure **ADD RENDERED FIGURE HERE**.

The analysis will be conducted by assuming the adhesion surface will be like a double lap joint, shown in Figure C.3 below.

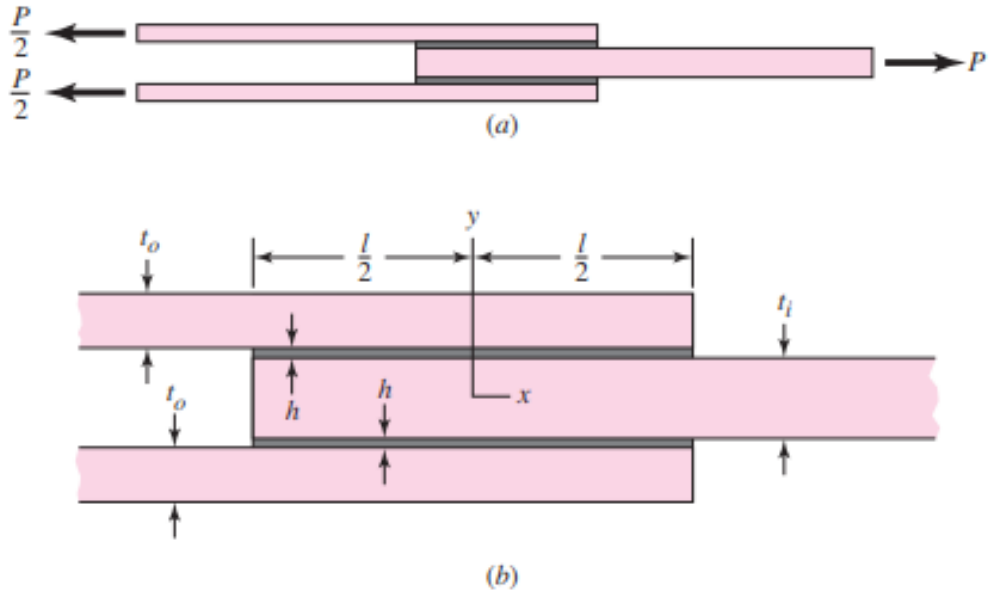


Figure C.3: Analysis of Carbon Fibre Adhesion (From Shigley's Machine Design [5, 484])

The shear-stress distribution of the joint is given by

$$\tau(x) = \frac{P\omega}{4bsinh(\omega l/2)}cosh(\omega x) + \left[\frac{P\omega}{4bcosh(\omega l/2)} \left(\frac{2E_0t_0 - E_it_i}{2E_0t_0 + E_it_i} \right) + \frac{(\alpha_i - \alpha_0)\Delta T\omega}{(1/E_0t_0 + 2/E_it_i)cosh(\omega l/2)} \right] sinh(\omega x) \quad (\text{C.9})$$

$$\omega = \sqrt{\frac{G}{h} \left(\frac{1}{E_0 t_0} + \frac{2}{E_i t_i} \right)} \quad (\text{C.10})$$

Where E_o , t_0 α_0 and E_i , t_i α_i are the modulus, thickness, coefficient of thermal expansion for the outer and inner adherend, respectively. G , h , b and l are the shear modulus, thickness, width and length of the adhesive, respectively. ΔT is the change in temperature of the joint, from its curing temperature (zero stress temperature). The closer the curing temperature of the adhesive is to the operating temperature, the lower the thermal stresses induced in the joint will be.

For this case, an unmodified epoxy will be selected as the adhesive material. From [5], Table 9-7, the lap-shear strength can be anywhere from $10.3 - 27.6 \text{ MPa}$. 10.3 MPa will be selected as a conservative estimate.

The outer material is aluminium and the inner material will be carbon fibre. Because of the nature of aluminium, an extremely thin layer of fibreglass should be added between the carbon fibre and aluminium to prevent corrosion due to the curing of the epoxy. Data was found as follows:

$$\begin{aligned} G &= 1.3 \text{ GPa} \quad [21] \\ E_i &= 109 \text{ GPa} \quad [16] \\ \alpha_i &= 23.7 * 10^{-6} \text{ mm/mm}^\circ\text{C} \quad [16] \\ E_0 &= 71 \text{ GPa} \quad [5] \\ \alpha_0 &= 23.94 \text{ mm/mm}^\circ\text{C} \quad [5] \end{aligned}$$

ΔT can be estimated by assuming the epoxy is cured at room temperature (20°C) and that the lowest temperature the blimp will be used at is -40°C . This yields $\Delta T = -60^\circ\text{C}$. The thickness of the adhesive will be estimated as $h = 0.5 \text{ mm}$. As preliminary estimates, $t_0 = 9.73 \text{ mm}$, $t_i = 9.73 \text{ mm}$, $l = 30 \text{ mm}$, and $b = 50.80 \text{ mm}$. The force P can be estimated using **SOME STUFF** $P = 100 \text{ N}$.

Substituting these values into Equation C.10 yields

$$\omega = \sqrt{\frac{1300 \text{ MPa}}{0.5 \text{ mm}} \left(\frac{1}{71000 \text{ MPa} * 9.73 \text{ mm}} + \frac{2}{109000 \text{ MPa} * 9.73 \text{ mm}} \right)} = 0.0930946 \text{ mm}^{-1} \quad (\text{C.11})$$

Followed by substitution into Equation C.9:

$$\begin{aligned}
 \tau(x) &= \frac{100N * 0.0930946mm^{-1}}{4 * 50.80mm * \sinh(0.0930946mm^{-1} * 30mm/2)} \cosh(0.0930946mm^{-1} * x) + \\
 &\left[\frac{100N * 0.0930946mm^{-1}}{4 * 50.80mm * \cosh(0.0930946mm^{-1} * 30mm/2)} \left(\frac{2 * 71000MPa * 9.73mm - 1300MPa * 9.73mm}{2 * 71000MPa * 9.73mm + 1300MPa * 9.73mm} \right) + \right. \\
 &\left. \frac{(23.7 * 10^{-6}mm/mm^{\circ}C - 23.94 * 10^{-6}mm/mm^{\circ}C) * (-60^{\circ}C) * 0.0930946mm^{-1}}{\left(\frac{1}{71000MPa * 9.73mm} + \frac{2}{109000MPa * 9.73mm} \right) \cosh(0.0930946mm^{-1} * 30mm/2)} \right] \sinh(0.0930946mm^{-1} * x) \\
 &= 0.02416MPa * \cosh(0.0930946mm^{-1} * x) + [0.02098MPa + 0.1871MPa] \sinh(0.0930946mm^{-1} * x)
 \end{aligned} \tag{C.12}$$

at $x = l/2 = 30mm/2$, the shear is at a maximum value. Therefore, the shear force is $\tau = 0.4464MPa$, Yielding a safety factor of $\eta = 10.3MPa/0.4464MPa = 23.0734$.

C.8 Thruster Bearings

C.9 Vectoring Shaft Screw Axial Loading Conditions

The screw which secures the nylon vectoring shaft is part of the servo motor assembly. The servo motor output is a spline with a female thread for a 3mm screw to be threaded into (Servo example from ServoCity [25]), as shown in Figure C.4.



Figure C.4: HS-7950TH Servo Spline Attachment [25]

One potential concern would be for the small 3mm screw (which threads into the spline) breaking if an axial load was applied to it. While there is *theoretically* no scenario where any axial load is applied, it is worth checking the strength of the screw, because during transportation of the airship it is possible that the

part may be unintentionally pulled. To find the proof force of the bolt, it was assumed that the bolt was a SAE Class 4.8 M3-0.5, and the following properties were found:

Table C.1: Table of Bolt Strength for a M3-0.5 Bolt [2]

| RESULTS | | | |
|---|-------------------|--------|---------------|
| Parameter | Symbol | Value | Unit |
| Designation | -- | M3x0.5 | --- |
| Property Class | - | 4.8 | |
| Screw Thread Series | -- | Coarse | |
| Nominal Stress Area | A_{s_nom} | 5.03 | mm^2 |
| Minimum Tensile Strength | R_m_{min} | 420 | MPa |
| Minimum Ultimate Tensile Load | - | 2110 | N |
| Minimum Stress at 0,2 % non-proportional elongation | $R_{p0.2}_{min}$ | --- | MPa |
| Stress Under Proof Load | s_p | 310 | |
| Proof Load | - | 1560 | N |
| Minimum Breaking Torque | M_B_{min} | --- | N.m |
| Vickers Hardness , $F \geq 98$ N | Minimum | 130 | HV |
| | Maximum | 220 | |
| Minimum Brinell Hardness , $F = 30 D^2$ | Minimum | 124 | HBW |
| | Maximum | 209 | |

Based on this, the tensile load of the bolt is 2110N, which is much higher than any axial forces that the shaft is expected to have to withstand. Therefore the design is not a problem.

C.10 Cauchy Stress Tensor [29]

The Cauchy Stress tensor fully defines the stresses acting on an infinitesimally small element within a material. It is particularly useful for failure analysis, as it is the internal stresses within a material that are used to determine the safety factor of the material at a specific location. Its general forms are shown below.

$$\sigma = \begin{bmatrix} \sigma_{11} & \sigma_{12} & \sigma_{13} \\ \sigma_{21} & \sigma_{22} & \sigma_{23} \\ \sigma_{31} & \sigma_{32} & \sigma_{33} \end{bmatrix} \equiv \begin{bmatrix} \sigma_{xx} & \sigma_{xy} & \sigma_{xz} \\ \sigma_{yx} & \sigma_{yy} & \sigma_{yz} \\ \sigma_{zx} & \sigma_{zy} & \sigma_{zz} \end{bmatrix} \equiv \begin{bmatrix} \sigma_x & \tau_{xy} & \tau_{xz} \\ \tau_{yx} & \sigma_y & \tau_{yz} \\ \tau_{zx} & \tau_{zy} & \sigma_z \end{bmatrix} \quad (\text{C.13})$$

Generally, the use of failure theories requires knowing the *principal stresses*. These are located perpendicular to the *principal planes*. Any body in a state of stress will have three principal planes, where there are no normal shear stresses, only three *principal stresses*.

Any stress tensor can undergo a change of coordinates to obtain the principal stresses. The transformed stress tensor can be written as follows:

$$\sigma' = \begin{bmatrix} \sigma_1 & 0 & 0 \\ 0 & \sigma_2 & 0 \\ 0 & 0 & \sigma_3 \end{bmatrix} \quad (\text{C.14})$$

Obtaining the principle stresses is relatively simple. The principle stresses are simply the eigenvalues of the stress tensor. MATLAB is used to find the eigenvalues of a given stress tensor, and the principle stresses are given by

$$\sigma_1 = \max(\lambda_1, \lambda_2, \lambda_3) \quad (\text{C.15})$$

$$\sigma_3 = \min(\lambda_1, \lambda_2, \lambda_3) \quad (\text{C.16})$$

$$\sigma_2 = \sigma_{11} + \sigma_{22} + \sigma_{33} - \sigma_1 - \sigma_3 \quad (\text{C.17})$$

The principal stresses are then used to conduct failure analysis using the preferred failure analysis method (e.g. Von Mises).

C.11 Previous Drag Analysis

Before knowing that the airship envelope needed to be parametrizable, drag values were initially computed using SolidWorks, by its built in Flow Simulation add-on. Simulations were conducted from 2m/s to 20m/s, at intervals of 2m/s. Skin Friction Drag and Regular Drag were computed and summed to obtain total drag for each speed. A table with the results from the simulations can be seen in Table C.2.

Table C.2: Raw Data From SolidWorks Flow Simulation

| Airspeed (m/s) | Drag Force (N) | Skin Friction Force (N) | Total Drag (N) |
|----------------|----------------|-------------------------|----------------|
| 2 | 0.4012 | 0.0651 | 0.4663 |
| 4 | 1.5286 | 0.2035 | 1.7320 |
| 6 | 3.1225 | 0.4011 | 3.5236 |
| 8 | 5.2179 | 0.7063 | 5.9242 |
| 10 | 8.2517 | 1.1397 | 9.3913 |
| 12 | 12.4647 | 2.0588 | 14.5235 |
| 14 | 17.4157 | 3.9501 | 21.3659 |
| 16 | 22.8193 | 5.3402 | 28.1595 |
| 18 | 29.0603 | 6.8692 | 35.9296 |
| 20 | 35.6981 | 8.4702 | 44.1682 |

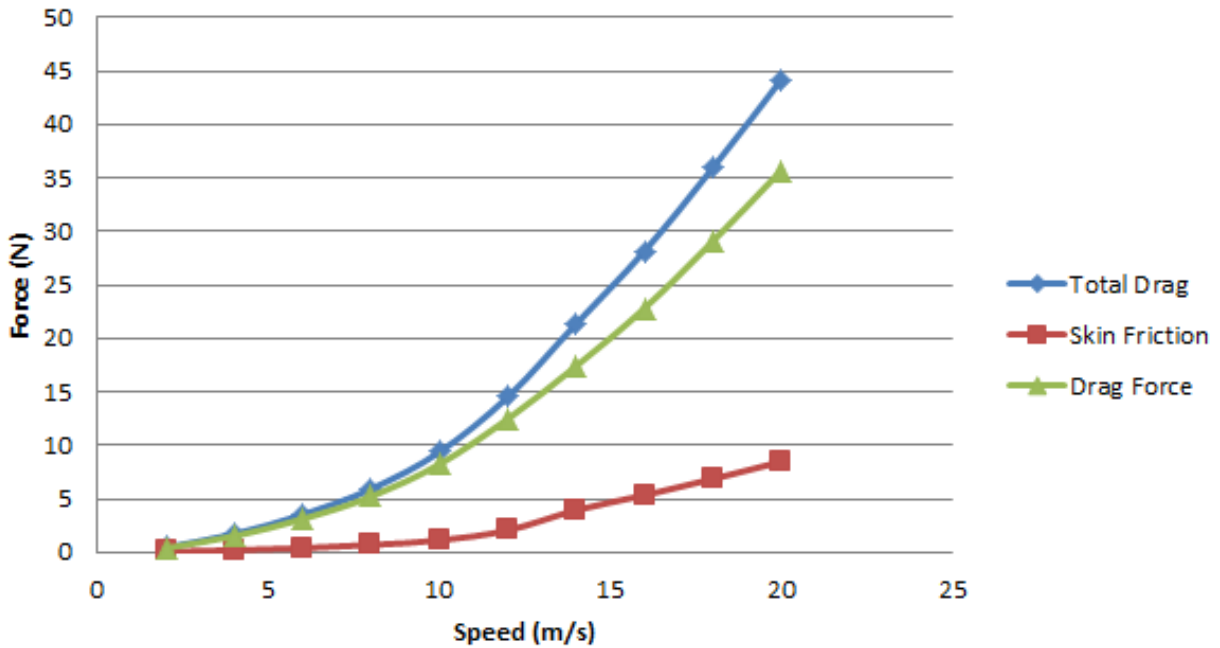


Figure C.5: Drag Force Curves Computed From SolidWorks Flow Simulation

The values of simulated drag were then sent into MATLAB and a curve fitting analysis was completed.

A graph of the raw data versus the fitted curve is shown in Figure C.5.

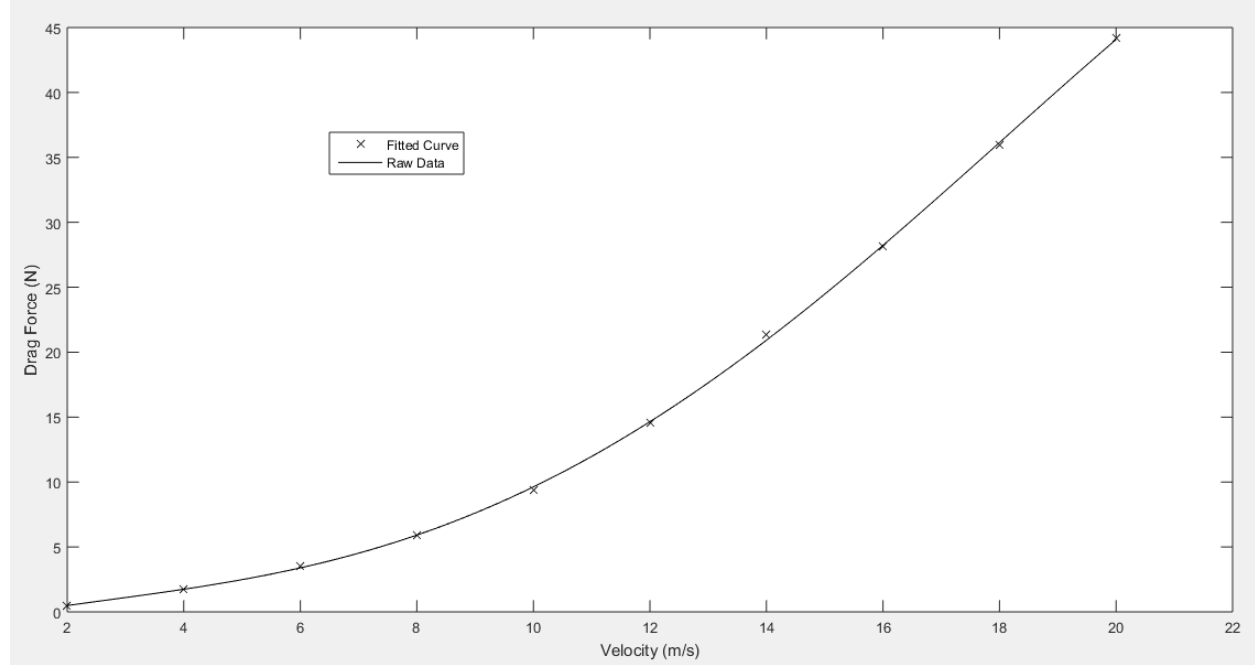


Figure C.6: Drag Force Curves Computed From SolidWorks Flow Simulation

The equation from the curve (generated from MATLAB) was found to be:

$$D(v) = -0.0003545v^4 + 0.014182v^3 - 0.05385v^2 + 0.45054v - 0.087259 \quad (\text{C.18})$$

Where D is the drag force and v is the airship speed, in m/s . Equation C.18 is what is used throughout the report to obtain drag forces.

Raw MATLAB code:

```

1 v=[0,2,4,6,8,10,12,14,16,18,20];
2 x=transpose(v);
3 d=[0,0.4663,1.7320,3.5236,5.9242,9.3913,14.5235,21.3659,28.1595,35.9296,44.1682];
4 y=transpose(d);
5 f=fit(x,y,'poly4');
6
7 cvalues = coeffvalues(f);
8 cnames = coeffnames(f);
9 output = formula(f);
10
11 for ii=1:1:numel(cvalues)
12     cname = cnames{ii};
13     cvalue = num2str(cvalues(ii));
14     output = strrep(output, cname, cvalue);

```

```

15 end
16
17 disp(output)
18
19 plot(f,'k',v,d,'xk'), xlabel('Velocity (m/s)'), ylabel('Drag Force (N)'), ...
20 legend('Fitted Curve', 'Raw Data')

```

C.12 New Drag Analysis

Once it was understood that the airship itself needed to be parametrizable, a new method of computed drag needed to be determined, as the simulations only accounted for the old airship dimensions. For this, an analysis from a report called *Technical Manual of Airship Aerodynamics* [28] was used. The following formula was used to compute drag:

$$D = C_D \rho (vol)^{2/3} v^{1.86} \quad (\text{C.19})$$

Where D is the drag in lbf (converted to N), ρ is the density of air [$slugs/ft^3$], vol is the volume of the airship envelope [ft^3], v is the velocity of the airship [ft/s], and C_D is the Prandtl Shape Coefficient. For this airship, C_D is estimated using Table C.3 below.

Table C.3: Airship Model Characteristics and Data [28]

| Name of model | Length, L | Diameter, D | Surface, S | Area maximum cross-sectional area A | Volume, Vol. | Prandtl shape coefficient, C_D | | | Fineness ratio $F_R = \frac{L}{D}$ | Distance maximum diameter from nose | Distance CG from nose | Prismatic coefficient, $Q = \frac{Vol.}{A \times L}$ | Index of form efficiency, $H_F = \frac{Q}{C_D}$ | | |
|-----------------------------------|----------------|------------------|-----------------|--|-----------------|-------------------------------------|-------------|-------------|---------------------------------------|-------------------------------------|-----------------------|---|--|-------------|-------------|
| | | | | | | 20 m. p. h. | 40 m. p. h. | 60 m. p. h. | | | | | 20 m. p. h. | 40 m. p. h. | 60 m. p. h. |
| Navy B (Goodrich) | 3. 527 | 0. 6967 | 5. 800 | 0. 381 | 0. 8304 | 0. 0168 | 0. 0154 | 0. 0148 | 5. 060 | 37. 80 | | 0. 6176 | 36. 76 | 40. 10 | 41. 73 |
| Navy C | 2. 919 | . 6417 | 4. 750 | . 323 | . 6259 | . 0159 | . 0144 | . 0136 | 4. 620 | 30. 00 | 46. 37 | . 6562 | 41. 27 | 45. 57 | 48. 25 |
| Navy E | 4. 125 | . 6417 | 5. 007 | . 323 | . 6690 | . 0168 | . 0146 | . 0142 | 4. 870 | 36. 25 | 48. 64 | . 6621 | | | |
| E. P. | 3. 092 | . 6417 | 4. 597 | . 323 | . 5890 | . 0166 | . 0147 | . 0138 | 4. 820 | 41. 59 | 43. 92 | . 6891 | 35. 49 | 40. 08 | 42. 70 |
| I. E. | 2. 985 | . 6417 | 4. 597 | . 323 | . 5955 | . 0175 | . 0155 | . 0144 | 4. 650 | 38. 18 | 44. 25 | . 6169 | 35. 25 | 39. 80 | 42. 84 |
| Goodyear-4 2 | 3. 190 | . 6870 | 5. 470 | . 371 | . 7840 | . 0162 | . 0144 | . 0134 | 4. 640 | 28. 76 | | . 6624 | 40. 89 | 45. 37 | 49. 43 |
| Goodyear-1 | 3. 420 | . 6660 | 5. 600 | . 348 | . 7360 | | | | . 0141 | 5. 130 | 34. 15 | | 6184 | | |
| Goodyear-2 | 3. 830 | . 6350 | 6. 000 | . 317 | . 7520 | | | | . 0141 | 6. 020 | 36. 14 | | 6194 | | |
| Goodyear-3 | 3. 670 | . 6150 | 5. 900 | . 297 | . 7760 | | | | . 0140 | 5. 970 | 36. 36 | | 7119 | | |
| Goodyear-4 | 3. 190 | . 6870 | 5. 470 | . 371 | . 7840 | | | | . 0153 | 4. 640 | 28. 76 | | 6624 | | |
| Astra-Torres | 3. 167 | . 6914 | 5. 190 | . 309 | . 6583 | . 0190 | . 0159 | . 0147 | 4. 583 | 33. 80 | 49. 08 | . 6590 | 34. 68 | 41. 45 | 44. 83 |
| Parseval P. I | 3. 942 | . 6417 | 5. 465 | . 323 | . 7240 | . 0185 | . 0174 | . 0165 | 6. 140 | 38. 75 | 43. 19 | . 5679 | 30. 70 | 32. 64 | 34. 42 |
| Parseval P. II | 3. 208 | . 6417 | 4. 528 | . 323 | . 5891 | . 0181 | . 0170 | . 0164 | 4. 990 | 38. 90 | 44. 46 | . 5677 | 31. 36 | 33. 39 | 34. 62 |
| Parseval P. III | 3. 208 | . 6417 | 4. 750 | . 323 | . 6331 | . 0179 | . 0169 | . 0161 | 4. 699 | 47. 33 | 45. 85 | . 6095 | 34. 05 | 36. 06 | 37. 86 |
| Parseval S. S. T | 5. 625 | 1. 1330 | 14. 720 | 1. 008 | 3. 4550 | . 0174 | . 0173 | . 0170 | 4. 960 | 45. 00 | 45. 88 | . 6090 | 35. 00 | 35. 23 | 35. 82 |
| Pony Blimp AA | 1. 992 | . 5833 | 2. 760 | . 267 | . 3196 | . 0205 | . 0254 | . 0277 | 3. 410 | 42. 50 | 46. 00 | . 6003 | 29. 28 | 23. 63 | 21. 67 |
| UB-FC | 4. 9383 | 1. 0591 | 12. 9584 | . 8810 | 2. 8693 | . 0321 | . 0223 | . 0219 | 4. 663 | | | . 65746 | | | |
| UB-2 | 4. 4894 | 1. 1638 | 12. 2240 | 1. 0633 | 2. 9201 | . 0205 | . 0189 | . 0192 | 3. 823 | | | . 61145 | | | |
| <i>C class cylindric midships</i> | | | | | | | | | | | | | | | |
| 1/4 diameter | 3. 109 | . 6417 | 5. 073 | . 323 | . 6777 | . 0154 | . 0140 | . 0132 | 4. 855 | | | . 6749 | 43. 82 | 48. 21 | 51. 13 |
| 1/2 diameter | 3. 270 | . 6417 | 5. 398 | . 323 | . 7297 | . 0153 | . 0141 | . 0135 | 5. 100 | | | . 6909 | 45. 16 | 49. 00 | 51. 18 |
| 1 diameter | 3. 590 | . 6417 | 6. 043 | . 323 | . 8330 | . 0164 | . 0146 | . 0136 | 5. 570 | | | . 7184 | 43. 80 | 49. 21 | 52. 82 |
| 2 diameter | 4. 232 | . 6417 | 7. 337 | . 323 | 1. 0404 | . 0175 | . 0150 | . 0136 | 6. 600 | | | . 7611 | 43. 49 | 50. 74 | 55. 96 |
| 3 diameter | 4. 872 | . 6417 | 8. 627 | . 323 | 1. 2471 | . 0173 | . 0156 | . 0148 | 7. 590 | | | . 7925 | 45. 81 | 50. 80 | 53. 55 |
| 4 diameter | 5. 515 | . 6417 | 9. 922 | . 323 | 1. 4548 | . 0175 | . 0157 | . 0146 | 8. 590 | | | . 8167 | 46. 67 | 52. 02 | 55. 94 |
| 5 diameter | 6. 158 | . 6417 | 11. 218 | . 323 | 1. 6625 | . 0164 | . 0154 | . 0148 | 9. 602 | | | . 8358 | 50. 96 | 54. 27 | 56. 47 |

Various airship dimensions can be seen below here. The aircraft dimensions shown below were for

testing done in a wind tunnel to determine drag effects on real airships, so they are scaled down models. The goal is to select a model that has comparable dimensions to the airship we are using. As a starting point, the fineness ratio f is computed for our airship. As an estimate, $f = L/D \approx 3.6/1.2 = 3$. In reference to Table C.3, the closest match would be the Pony Blimp AA, with a fineness ratio of 3.4.

It can be deduced from the table that the Prandtl Shape coefficient encompasses both skin and form drag. When the fineness ratio is higher, skin friction drag will have a larger effect than form drag, so when the airspeed is increased (from 20mph to 60mph), C_D will decrease. The opposite is true with small fineness ratios, where the form drag plays a larger role, therefore the C_D increases as airspeed is increased. To be conservative, the highest C_D from the Pony Blimp AA, therefore $C_D = 0.0227$. An example calculation is shown below, for a windspeed of $20m/s$:

$$D = C_D \rho (vol)^{2/3} v^{1.86} = 0.0227 * (0.00237 \text{ slugs}/ft^3) * (122.644 ft^3)^{2/3} (65.616 ft/s)^{1.86} = 3.183 lb f = 14.1586 N \quad (\text{C.20})$$

The formula will be converted into metric units for simplicity, using a multiplication factor.

$$D = 0.847103 * (C_D) * (\rho [kg/m^3]) * (vol[m^3])^{2/3} * (v[m/s])^{1.86} \quad (\text{C.21})$$

Based on Table C.4, the envelope contributes 45% to the drag. Therefore the total drag will be estimated as $D_{total} = D/0.45$. Based on this, the total drag is found in Equation C.20 is now $31.463 N$

Table C.4: Drag Contribution for Various Airship Components [28]

| (1) Large nonrigids with closed cars: | | <i>Percent</i> |
|---------------------------------------|-------------------------------|----------------|
| (a) | Envelope | 45 |
| (b) | Surfaces | 20 |
| (c) | Rigging and suspension cables | 15 |
| (d) | Cars | 15 |
| (e) | Accessories | 5 |
| (2) Small nonrigids with open cars: | | |
| (a) | Envelope | 35 |
| (b) | Surfaces | 25 |
| (c) | Rigging and cables | 20 |
| (d) | Cars | 15 |
| (e) | Accessories | 5 |

The value of C_D will change based on the fineness ratio. In the GUI of the MATLAB program, the user will select a fineness ratio from a drop-down menu, of 3.5, 4, and 4.5, followed by a total length of the blimp. To calculate the drag for these situations, the volume of the blimp will be computed, and the C_D will change based on the fineness ratio, as follows:

Table C.5: Fineness Ratios and Corresponding C_D

| Fineness Ratio | C_D |
|----------------|-------|
| 3.5 | 0.254 |
| 4 | 0.189 |
| 4.5 | 0.159 |

C.13 Thrust Force

Vectoring thrusters will be mounted to the both sides of the airship via the thruster supports attached to the keel. In order to encompass the forces that will be generated by the thruster, an equation will be used which was developed via research and experimental data collected and compiled by Gabriel Staples [27]. The basis of the equation is Newtons second law.

$$T = \frac{\partial(mv)}{\partial t} = \dot{m}v$$

based on this equation, in theory static thrust can be defined as

$$T_{static} = \dot{m}V_e$$

where V_e is the escape velocity of air through the thruster in m/s and \dot{m} is the mass flow of air through the thruster in kg/s . For dynamic thrust, which incorporates the movement of the airship,

$$T = \dot{m}\Delta V = \dot{m}(V_e - V_{as})$$

where V_{as} is the velocity of air coming into the thrusters in m/s but in a windless circumstance it is the airship velocity. Knowing that $\dot{m} = \rho A V_e$ and $A = \pi \frac{D^2}{4}$ where A is the area the propellers will cover in m^2 and D is the diameter of the propellers in m .

$$T = \rho \frac{\pi D^2}{4} (V_e^2 - V_e V_{as}) \quad (C.22)$$

There is obviously some proportionality between the escape velocity V_e and the tip velocity of the propeller. This claim can be supported by the fact that the tangential velocity of a propeller blade will be increasing along its radius, therefore the greater the diameter the higher the tip speed. This velocity will affect the incident velocity of air it comes into contact with. Therefore a greater diameter will result in greater thrust as well as higher efficiency compared to a propeller of the same pitch with a lesser diameter [27]. This effect however tops out when the tip speed approaches the speed of sound.

Pitch will also affect both the thrust and efficiency. Lower pitch diameter results in lower angle of attack. Lower angle of attack means less separation, less induced drag, as a result, higher diameter and lower pitch props will typically be more efficient [27].

In order to incorporate this into equation C.22, V_e is replaced with V_{pitch} which equals $RPM \cdot Pitch \cdot \frac{1min}{60s}$ where RPM is the rotations per minute of the motor, and $Pitch$ is the pitch diameter of the propeller blade in m . Equation C.22 is multiplied by a constant coefficient and the propeller diameter to pitch ratio to the power of a constant, as seen below in equation C.23.

$$T = \rho \frac{\pi D^2}{4} \left(K_1 \left(\frac{D}{Pitch} \right)^{K_2} \right) \left(\left(RPM \cdot Pitch \cdot \frac{1min}{60s} \right)^2 - V_{as} \left(RPM \cdot Pitch \cdot \frac{1min}{60s} \right) \right) \quad (\text{C.23})$$

The assumption that $V_e \approx V_{pitch}$ is not accurate. In addition, it is assumed that the air velocity across the area of the thruster will be constant, when in reality this is not the case [27]. Some of the error derived from these assumptions is corrected by the coefficient term in C.23. In order to choose these coefficients, a study done by Gabriel Staples [27] [26], compares data calculated with equation C.23 using varying constants, with experimental static thrust data from more than 150 tests which were done by multiple sources. These were used along with theoretical dynamic thrust data [4], and a smaller sample of experimental dynamic thrust data. The values for K_1 and K_2 that resulted in calculated thrust forces that best matched the experimental data were 0.16716 and 1.5. Since these values were determined using mainly static thrust data, they are more accurate when calculating static thrust. The highest forces will be generated during low speed or static thrusting so these will be the values used when modeling the parts supporting the thrusters. Results from comparing thrust values calculated using Gabriel Staples's equation C.24 and experimental data for both static and dynamic thrust can be found in appendix section C.13, Figures C.8 and C.9.

The following equation shows a sample calculation using an achievable motor RPM of 11000 from the HobbyKing 2612 Brushless Outrunner Motor 1900KV, whose specs can be seen in appendix section D.6.1. This RPM value was based off results obtained from an online calculator comparing required power values at varying RPMs to the power shown in appendix section C.13, Figures C.10. An airship speed of 10m/s was used.

$$T = \rho \frac{\pi D^2}{4} \left(0.16716 \left(\frac{D}{Pitch} \right)^{1.5} \right) \left(\left(RPM \cdot Pitch \cdot \frac{1min}{60s} \right)^2 - V_{as} \left(RPM \cdot Pitch \cdot \frac{1min}{60s} \right) \right) \quad (\text{C.24})$$

$$\begin{aligned} &= 1.225[kg/m^3] \frac{\pi(0.1778[m])^2}{4} \left(0.16716 \left(\frac{0.1778[m]}{0.127[m]} \right)^{1.5} \right) \left(\left(11000[rpm] \cdot 0.127[m] \cdot \frac{1min}{60s} \right)^2 \right. \\ &\quad \left. - 10[m/s] \left(11000[rpm] \cdot Pitch \cdot \frac{1min}{60s} \right) \right) = 2.604[N] \end{aligned}$$

Appendix section C.13, Figure C.7 depicts the decrease in thrust force with increasing airship speed. This phenomena can also be observed below in table C.6. At and RPM of 11000 as the air ship reaches 24m/s the thrust force goes to 0 indicating that this would be the maximum speed. Obviously there are several considerable forces such as gravitational forces, drag, and other aerodynamic forces which are not accounted and this is therefore not an accurate method of determining maximum speed.

Table C.6: Table of Calculated Thrust Values for Varying Airship Speeds

| Airship Speed, V_{as} , (m/s) | Airship Speed, V_{as} (mph) | Thrust, T (N) | Thrust, T (g) | Thrust, T (kg) |
|---------------------------------|-------------------------------|---------------|---------------|----------------|
| 0 | 0.000 | 4.566 | 465.403 | 0.465 |
| 1 | 2.237 | 4.370 | 445.414 | 0.445 |
| 2 | 4.474 | 4.173 | 425.425 | 0.425 |
| 3 | 6.711 | 3.977 | 405.436 | 0.405 |
| 4 | 8.948 | 3.781 | 385.448 | 0.385 |
| 5 | 11.185 | 3.585 | 365.459 | 0.365 |
| 6 | 13.422 | 3.389 | 345.470 | 0.345 |
| 7 | 15.659 | 3.193 | 325.482 | 0.325 |
| 8 | 17.896 | 2.997 | 305.493 | 0.305 |
| 9 | 20.132 | 2.801 | 285.504 | 0.286 |
| 10 | 22.369 | 2.605 | 265.516 | 0.266 |
| 11 | 24.606 | 2.409 | 245.527 | 0.246 |
| 12 | 26.843 | 2.213 | 225.538 | 0.226 |
| 13 | 29.080 | 2.016 | 205.550 | 0.206 |
| 14 | 31.317 | 1.820 | 185.561 | 0.186 |
| 15 | 33.554 | 1.624 | 165.572 | 0.166 |
| 16 | 35.791 | 1.428 | 145.584 | 0.146 |
| 17 | 38.028 | 1.232 | 125.595 | 0.126 |
| 18 | 40.265 | 1.036 | 105.606 | 0.106 |
| 19 | 42.502 | 0.840 | 85.617 | 0.086 |
| 20 | 44.739 | 0.644 | 65.629 | 0.066 |
| 21 | 46.976 | 0.448 | 45.640 | 0.046 |
| 22 | 49.213 | 0.252 | 25.651 | 0.026 |
| 23 | 51.450 | 0.056 | 5.663 | 0.006 |
| 24 | 53.687 | -0.141 | -14.326 | -0.014 |

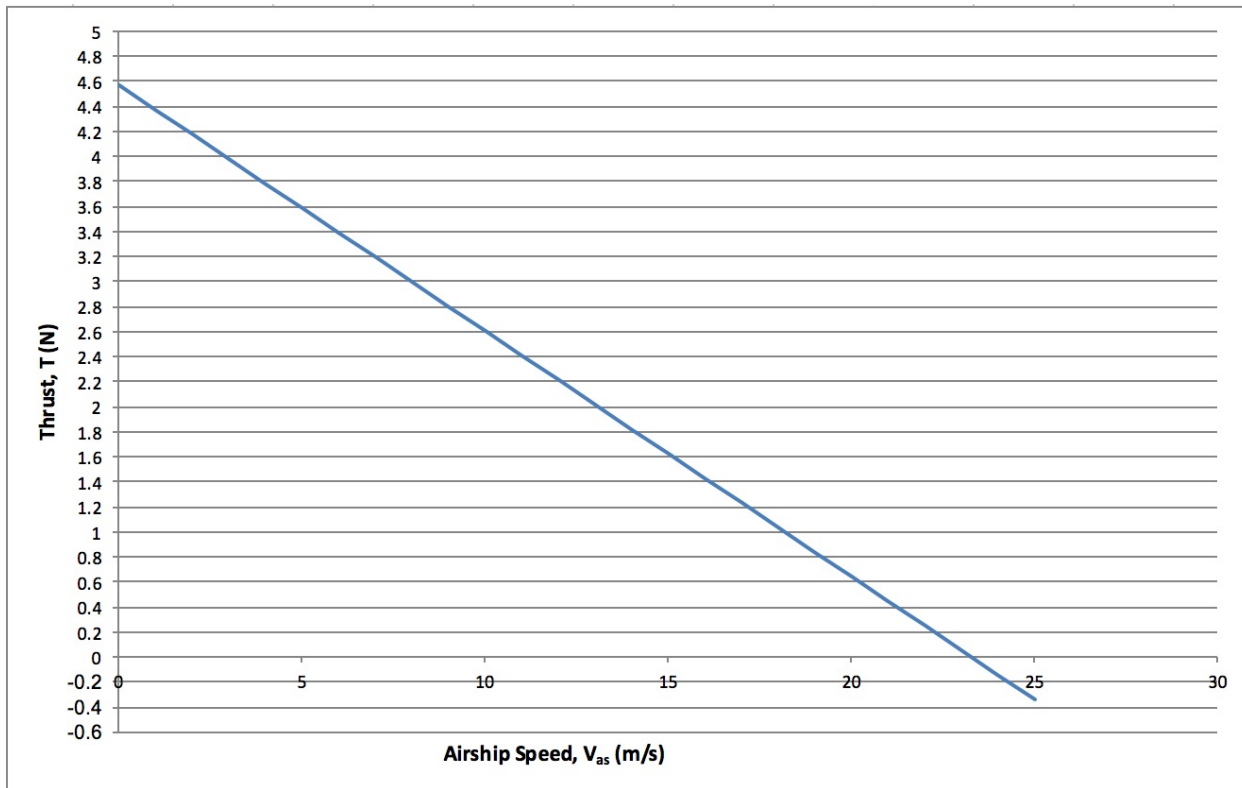


Figure C.7: Graph of Thrust Plotted Against Airship Speed at 11000rpm With 7", 5" Pitch Diameter Propeller

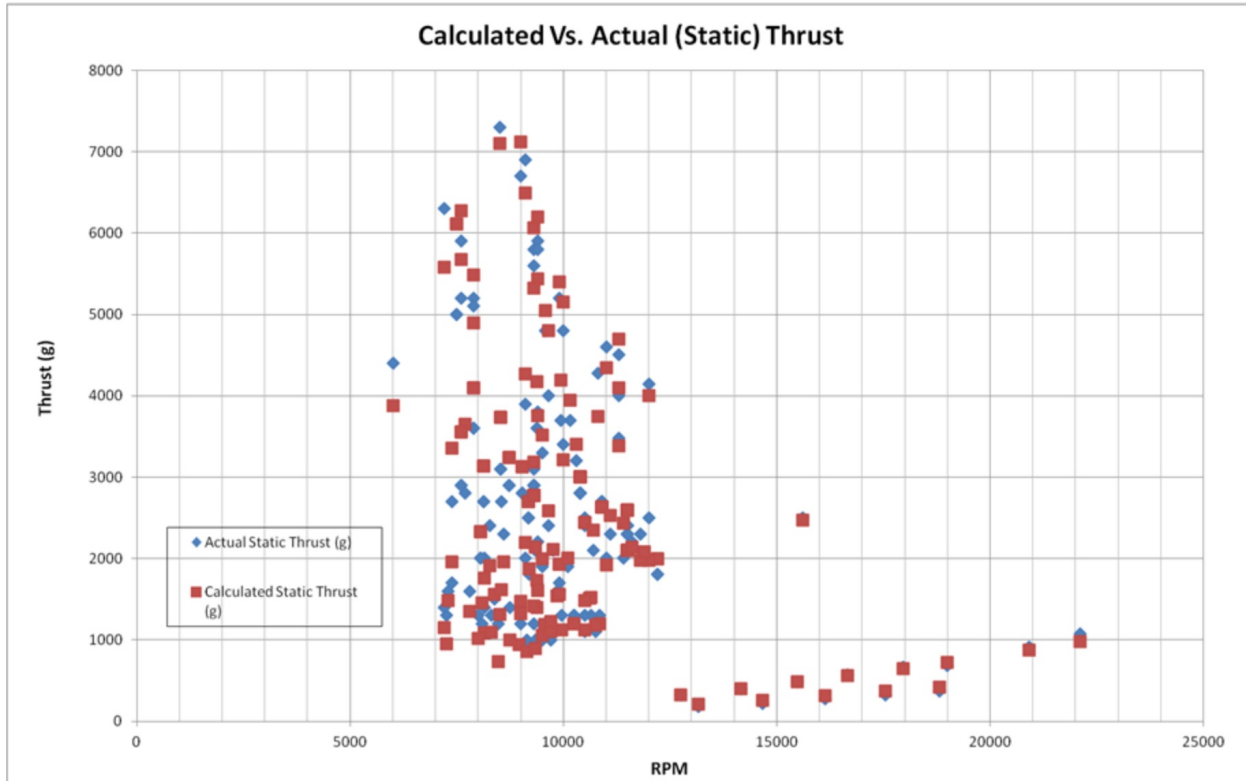


Figure C.8: Test Data from Gabriel Staples Against Experimental Static Thrust Values [27]

Propeller Dynamic Thrust - Experimental Results vs. Semi-empirical Calculation

10x6 propeller, Full Throttle

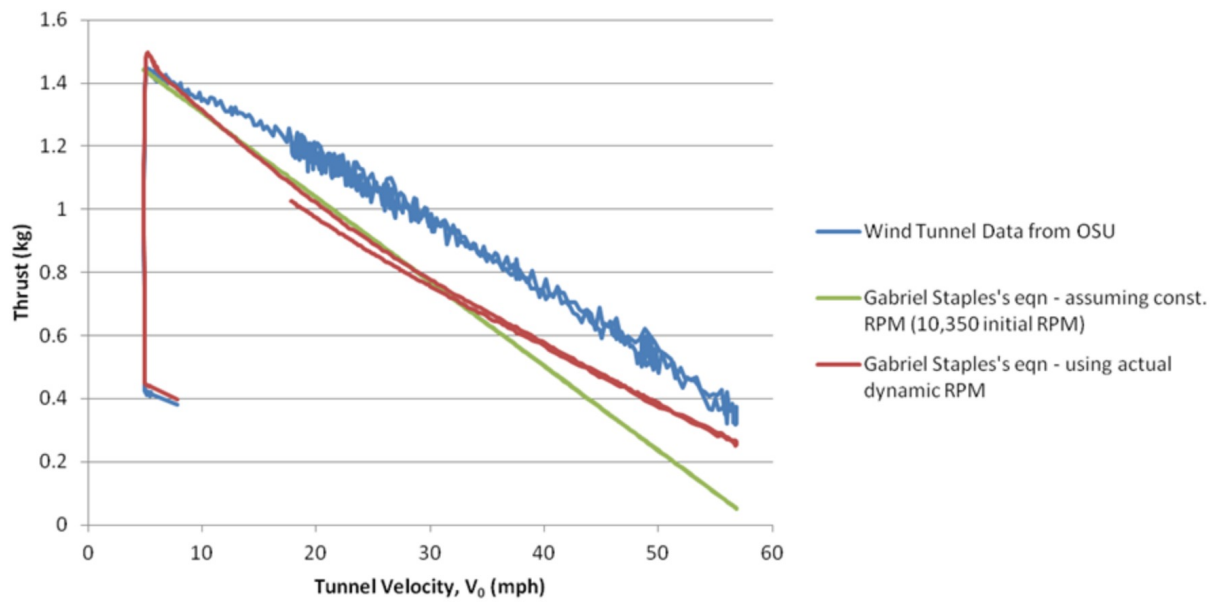


Figure C.9: Test Data from Gabriel Staples Against Experimental Dynamic Thrust Values [27]

| | | |
|---|---|----------------------------------|
| Propeller diameter | 7 | inch |
| Pitch | 5 | inch |
| Propeller type | Standard propeller <input type="button" value="▼"/> | |
| | CF | <input type="button" value="1"/> |
| No. of blades | 2 | <input type="button" value="▼"/> |
| RPM | 11000 | |
| Air temperature | 68 Fahrenheit <input type="button" value="▼"/> | |
| Air density | 1.2045 (kg/m ³) | |
| Static thrust = 12.34 oz | | |
| Static thrust = 0.79 pound | | |
| Static thrust = 0.35 kg | | |
| Perimeter speed = 102.35 m/s | | |
| Required engine power = 0.108 HP = 0.079 kW | | |
| Estimated flying speed = 52.0 mph = 45.1 Knots | | |

Figure C.10: Sample Thrust Calculation Using On-line Calculator [6]

Appendix D: Data Sheets

D.1 Linear Actuator [1]



100mm L12 Actuator
Actual Size

Benefits

- Compact
- Simple control
- Low voltage
- Equal push/pull
- Easy mounting

Applications

- Robotics
- Appliances
- Toys
- RC vehicles
- Automotive
- Industrial Automation

Miniature Linear Motion Series · L12

Actuonix Motion Devices unique line of Miniature Linear Actuators enables a new generation of motion-enabled product designs, with capabilities that have never before been combined in a device of this size. These small linear actuators are a superior alternative to designing with awkward gears, motors, servos, and linkages.

Actuonix's L series of micro linear actuators combine the best features of our existing micro actuator families into a highly flexible, configurable, and compact platform with an optional sophisticated on-board microcontroller. The first member of the L series, the L12, is an axial design with a powerful drive-train and a rectangular cross section for increased rigidity. But by far the most attractive feature of this actuator is the broad spectrum of available configurations.

L12 Specifications

| Gearing Option | 50:1 | 100:1 | 210:1 |
|---------------------------------------|---------------------------|--------------|---------------|
| Peak Power Point | 17N @ 14mm/s | 31N @ 7mm/s | 62N @ 3.2mm/s |
| Peak Efficiency Point | 10N @ 19mm/s | 17N @ 10mm/s | 36N @ 4.5mm/s |
| Max Speed (<i>no load</i>) | 25mm/s | 13mm/s | 6.5mm/s |
| Max Force (<i>lifted</i>) | 22N | 42N | 80N |
| Back Drive Force (<i>static</i>) | 12N | 22N | 45N |
| Stroke Option | 10 mm | 30mm | 50mm |
| Mass | 28 g | 34 g | 40 g |
| Repeatability (-I, -R, -P&LAC) | ±0.1 mm | ±0.2 mm | ±0.3 mm |
| Max Side Load (<i>extended</i>) | 50N | 40N | 30N |
| Closed Length (<i>hole to hole</i>) | 62mm | 82mm | 102mm |
| Potentiometer (-I, -R, -P) | 1kΩ±50% | 3kΩ±50% | 6kΩ±50% |
| Voltage Option | 6VDC | 12VDC | |
| Max Input Voltage | 7.5V | 13.5V | |
| Stall Current | 460mA | 185mA | |
| Standby Current (-I/-R) | 7.2mA | 3.3mA | |
| Operating Temperature | -10°C to +50°C | | |
| Potentiometer Linearity | Less than 2.00% | | |
| Max Duty Cycle | 20 % | | |
| Audible Noise | 55dB @ 45cm | | |
| Ingress Protection | IP-54 | | |
| Mechanical Backlash | 0.2mm | | |
| Limit Switches (-S) | Max. Current Leakage: 8uA | | |
| Maximum Static Force | 200N | | |

1 - Control Option Specific values are identified with -I, -R, -P, -S, and LAC

2 - 1 N (Newton) = 0.225 lbf (pound-force) & 25.4mm=1 Inch

3 - A powered-off actuator will statically hold a force up to the Backdrive Force

4 - Actuators should be tested in each specific application to determine their effective life under those loading conditions and environment.

All information provided on this datasheet is subject to change. Purchase or use of Actuonix actuators is subject to acceptance of our terms and conditions as posted here: <http://www.actuonix.com/terms.asp>



Actuonix Motion Devices Inc

580 Starling Lane

Victoria, BC, V9E 2A9

Canada

1(206) 347-9684 phone

1(888) 225-9198 toll-free

1(206) 347-9684 fax

sales@actuonix.com

Copyright 2016 © Actuonix Motion Devices Inc.

D.2 Bearings [18]

10/10/2017

McMaster-Carr - General Purpose Plastic Ball Bearing, with Stainless Steel Ball, for 1/4" Shaft Diameter, 5/8" OD



General Purpose Plastic Ball Bearing with Stainless Steel Ball, for 1/4" Shaft Diameter, 5/8" OD

In stock
\$6.03 Each
6455K2



| | |
|----------------------------|-------------------|
| Bearing Type | Ball |
| For Load Direction | Radial |
| Ball Bearing Type | Standard |
| Construction | Single Row |
| Seal Type | Open |
| For Shaft Shape | Round |
| Trade No. | R4 |
| For Shaft Diameter | 1/4" |
| ID | 0.25" |
| ID Tolerance | 0" to 0.003" |
| OD | 5/8" |
| OD Tolerance | -0.003" to 0" |
| Width | 0.196" |
| Width Tolerance | -0.005" to 0.005" |
| Material | Acetal |
| Cage Material | Plastic |
| Radial Load Capacity, lbs. | |
| Dynamic | 25 |
| Static | 15 |
| Maximum Speed | 2,300 rpm |
| Shaft Mount Type | Press Fit |
| Lubrication | Not Required |
| Temperature Range | -40° to 180° F |
| ABEC Rating | Not Rated |
| Radial Clearance | 0.001" to 0.008" |
| Ball Material | Stainless Steel |
| RoHS | Compliant |

Choose these acetal bearings for their all-around corrosion and chemical resistance.

Stainless steel balls offer excellent corrosion resistance.

D.3 Friction Wheel Assembly

D.3.1 Friction Wheel [17]

10/10/2017

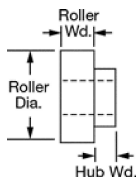
McMaster-Carr - Neoprene Roller, Drive, Aluminum Hub, 5/8" Roller Diameter, 3/16" Roller Width



Neoprene Roller

Drive, Aluminum Hub, 5/8" Roller Diameter, 3/16" Roller Width

In stock
\$16.70 Each
60885K31



| | |
|-----------------------------|--|
| Guide Roller Type | Drive |
| Roller Style | Shaft Mount |
| Roller Profile | Flat |
| Roller Material | Neoprene |
| Hub Material | Aluminum |
| Roller | |
| Diameter | 5/8" |
| Width | 3/16" |
| For Shaft Diameter | 1/4" |
| Hub | |
| Diameter | 1/2" |
| Width | 1/4" |
| Shaft Mount Type | Set Screw |
| Set Screws | |
| Number Required | 1 |
| Included | No |
| Thread Size | 8-32 |
| Temperature Range | -40° to 170° F |
| Durometer (Hardness Rating) | 55A (Medium) Black |
| RoHS | Compliant |
| Related Product | 8-32 Stainless Steel Cup Point Set Screws (100/Pkg.) |

Made of neoprene rubber, these rollers resist oil, flames, gasoline, and weather. Also known as contact wheels and feed rollers, they have tapped hubs that allow you to mount them onto a shaft or stud to transmit power.

D.3.2 Friction Wheel Set Screw [19]

10/10/2017

McMaster-Carr - Alloy Steel Cup-Point Set Screw, Black Oxide, 8-32 Thread, 1/4" Long



Alloy Steel Cup-Point Set Screw
Black Oxide, 8-32 Thread, 1/4" Long

In stock
\$10.65 per pack of 100
91375A190



| | |
|-------------------------------|-------------------------|
| Material | Black-Oxide Alloy Steel |
| Thread Size | 8-32 |
| Length | 1/4" |
| Drive Size | 5/64" |
| Screw Size Decimal Equivalent | 0.164" |
| Hardness | Rockwell C45 |
| Specifications Met | ASME B18.3, ASTM F912 |
| Thread Type | UNC |
| Thread Spacing | Coarse |
| Thread Fit | Class 3A |
| Thread Direction | Right Hand |
| Drive Style | Hex |
| Tip Type | Cup |
| Head Type | Headless |
| System of Measurement | Inch |
| RoHS | Compliant |

Made from alloy steel, these set screws have a thin edge that digs into hard surfaces for a secure hold. Length listed is the overall length.

Black-oxide alloy steel set screws resist corrosion in dry environments.

D.3.3 Friction Wheel Motor [22]

10/10/2017

Pololu - 50:1 Micro Metal Gearmotor HP 6V

50:1 Micro Metal Gearmotor HP 6V



www.pololu.com

Pololu item #: 998 438 in stock

| Price break | Unit price (US\$) |
|-------------|-------------------|
| 1 | 15.95 |
| 10 | 13.55 |
| 50 | 11.96 |

Quantity: Add to cart[backorders allowed](#) Add to wish list

This gearmotor is a miniature **high-power, 6 V** brushed DC motor with a **51.45:1** metal gearbox. It has a cross section of 10 × 12 mm, and the D-shaped gearbox output shaft is 9 mm long and 3 mm in diameter.

Key specs at 6 V: 625 RPM and 120 mA with no load, 15 oz-in (1.1 kg-cm) and 1.6 A at stall.

Select options:

[Description](#) [Specs \(10\)](#) [Pictures \(20\)](#) [Resources \(12\)](#) [FAQs \(1\)](#) [On the blog \(1\)](#)

Dimensions

| | |
|------------------------|------------------------------|
| Size: | 10 × 12 × 26 mm ¹ |
| Weight: | 9.5 g |
| Shaft diameter: | 3 mm ² |

General specifications

| | |
|-------------------------------|----------|
| Gear ratio: | 51.45:1 |
| Free-run speed @ 6V: | 630 rpm |
| Free-run current @ 6V: | 120 mA |
| Stall current @ 6V: | 1600 mA |
| Stall torque @ 6V: | 15 oz·in |
| Extended motor shaft?: | N |

<https://www.pololu.com/product/998/specs>

1/2

Table D.1: Various Gearing For Gondola Motor Torque [22].

| | | | | | | |
|------------|---|---------|----------|-----------|---------------------|--------------------------------|
| 6 V | high-power (HP) <i>(same specs as 6V HPCB above)</i> | 1600 mA | 6000 RPM | 2 oz-in | <u>5:1 HP 6V</u> | <u>5:1 HP 6V dual-shaft</u> |
| | | | 3000 RPM | 4 oz-in | <u>10:1 HP 6V</u> | <u>10:1 HP 6V dual-shaft</u> |
| | | | 1000 RPM | 9 oz-in | <u>30:1 HP 6V</u> | <u>30:1 HP 6V dual-shaft</u> |
| | | | 625 RPM | 15 oz-in | <u>50:1 HP 6V</u> | <u>50:1 HP 6V dual-shaft</u> |
| | | | 400 RPM | 22 oz-in | <u>75:1 HP 6V</u> | <u>75:1 HP 6V dual-shaft</u> |
| | | | 320 RPM | 30 oz-in | <u>100:1 HP 6V</u> | <u>100:1 HP 6V dual-shaft</u> |
| | | | 200 RPM | 40 oz-in | <u>150:1 HP 6V</u> | <u>150:1 HP 6V dual-shaft</u> |
| | | | 140 RPM | 50 oz-in | <u>210:1 HP 6V</u> | <u>210:1 HP 6V dual-shaft</u> |
| | | | 120 RPM | 60 oz-in | <u>250:1 HP 6V</u> | <u>250:1 HP 6V dual-shaft</u> |
| | | | 100 RPM | 70 oz-in | <u>298:1 HP 6V</u> | <u>298:1 HP 6V dual-shaft</u> |
| | | | 32 RPM | 125 oz-in | <u>1000:1 HP 6V</u> | <u>1000:1 HP 6V dual-shaft</u> |

D.3.4 Friction Wheel Encoder [23]

10/10/2017

Pololu - Magnetic Encoder Pair Kit for Micro Metal Gearmotors, 12 CPR, 2.7-18V (HPCB compatible)

Magnetic Encoder Pair Kit for Micro Metal Gearmotors, 12 CPR, 2.7-18V (HPCB compatible)

Pololu item #: 3081 **574** in stock

| Price break | Unit price (US\$) |
|-------------|-------------------|
| 1 | 8.95 |
| 10 | 7.95 |
| 50 | 6.95 |

Quantity: **Add to cart**

backorders allowed **Add to wish list**

Navigation icons: back, forward, search.

Add quadrature encoders to your micro metal gearmotors (extended back shaft version required) with this kit that uses a magnetic disc and hall effect sensors to provide 12 counts per revolution of the motor shaft. The sensors operate from 2.7 V to 18 V and provide digital outputs that can be connected directly to a microcontroller or other digital circuit. This module is compatible with **all** of the dual-shaft micro metal gearmotors we carry, including the HPCB versions.

[Description](#) [Specs \(6\)](#) [Pictures \(13\)](#) [Resources \(5\)](#) [FAQs \(0\)](#) [On the blog \(4\)](#)

Overview

This kit includes two dual-channel Hall Effect sensor boards and two **6-pole magnetic discs** that can be used to add quadrature encoding to two **micro metal gearmotors with extended back shafts** (motors are not included with this kit). The encoder board senses the rotation of the magnetic disc and provides a resolution of 12 counts per revolution of the motor shaft when counting both edges of both channels. To compute the counts per revolution of the gearbox output shaft, multiply the gear ratio by 12.

D.4 Spring [20]

10/10/2017

McMaster-Carr - Music-Wire Steel Torsion Spring, 180 Degree Right-Hand Wound, 0.767" OD



Music-Wire Steel Torsion Spring 180 Degree Right-Hand Wound, 0.767" OD

In stock
\$8.06 per pack of 6
9271K271



| Spring Type | Torsion |
|--------------------------------|------------------|
| Material | Music-Wire Steel |
| Deflection Angle | 180° |
| Wind Direction | Right Hand |
| OD | 0.767" |
| For Maximum Shaft Diameter | 0.500" |
| Wire Diameter | 0.063" |
| Leg Length | 2,000" |
| Number of Coils | 6.00 |
| Spring Length @ Maximum Torque | 0.475" |
| Maximum Torque | 5,518 in.-lbs. |
| RoHS | Compliant |

These music-wire steel springs are stronger than stainless steel springs. Commonly found in clothespins, spring clamps, mousetraps, motors, and spring-return mechanisms, torsion springs maintain pressure over a short distance in a rotational direction. They are often supported by a shaft, mandrel, or arbor.

Squeezing a torsion spring reduces its OD, which tightens the spring around a shaft and increases the spring length. Since the spring gets tighter as it is squeezed around the shaft, a maximum shaft diameter for each spring is listed. Using a shaft with a larger diameter will interfere with the spring motion.

Torsion springs should be used in the direction in which the coils are wound. Deflection angle represents the angle between the legs of the spring as well as the maximum spring rotation. All springs rotate until their legs are parallel. For example, a spring with a 90° deflection angle has a 90° angle between its legs, and it will rotate a maximum of 90°. Maximum torque is the torque required to rotate the spring legs to the parallel position.

D.5 Battery [7]

Rhino 2250mAh 3S 11.1v 40C Lipoly Pack



Specifications

| | | | |
|---------------------|------------|-----------------|--------|
| SKU: | R2250-40-3 | Brand: | N/A |
| Weight(g) | 243.00 | Length | 109.00 |
| Width: | 26.00 | Height: | 36.00 |
| Capacity (mAh) | 2250.00 | Discharge(c) | 40.00 |
| Length-A(mm): | 107.00 | Height-B(mm): | 34.00 |
| Width-C(mm) | 26.00 | Unit Weight (g) | 191 |
| Max Charge Rate(C): | 5.00 | Discharge Plug: | N/A |

D.6 Thruster Assembly

D.6.1 Thruster Motor [14]

HobbyKing®™ 2612 Brushless Outrunner 1900KV



Specifications

RPM/V: **1900Kv**
Cell Count: **2~3s Lipoly**
Max.efficiency: **78.0%**
Current at Max.eff: **6.3~8.7A**
Max.current: **14A**
No Load Current: **0.8A/7V**
Internal Resistance: **165mOhm**
Diameter: **27mm**
Length: **23.4mm**
Mounting Hole Spacings: **32mm**
Mounting Hole Diameter: **2mm**
Shaft: **3mm**
Weight: **25g**

D.6.2 Propeller [12]

Aerostar Carbon Fibre Propeller 7x5



Specifications

| | | | |
|-------------------|--------------|------------------|--------------|
| SKU: | 9445000180-0 | Brand: | N/A |
| Weight(g) | 14.00 | Length | 180.00 |
| Width: | 15.00 | Height: | 20.00 |
| Pitch Y(inch) | 5.00 | Material | Carbon Fiber |
| Rotation: | CCW | Unit Weight (g): | N/A |
| Type | Normal | Blade Count | 2 |
| Diameter X(inch): | 7.00 | | |

D.6.3 BEC [8]

TURNIGY Plush 10amp Speed Controller w/BEC



Specifications

| | | |
|---------------------------|-----------|---------|
| Cont Current: 10A | SKU: | TR_P10A |
| Burst Current: 12A | Weight(g) | 20.00 |
| BEC Mode: Linear | Width: | 10.00 |
| BEC : 5v / 2A | Brand: | No |
| Lipo Cells: 2-4 | Length | 110.00 |
| NiMH : 5-12 | Height: | 110.00 |
| Weight: 9g | | |
| Size: 27x17x6mm | | |

D.6.4 Servo Motor [24]

RB-Hit-128

HS-7950TH Ultra Torque HV Coreless Titanium Gear Servo



Hitec's strongest servo period, the "Ultra Torque" HS-7950TH is designed to operate on a two cell LiPo Pack. Featuring our high resolution "G2" second generation programmable digital circuit and our indestructible Titanium gears, the HS-7950TH has the performance and durability you've come to expect from a Hitec servo. Other features in the HS-7950TH include a 7.4V optimized coreless motor, integrated heat sink case, and a top case with two hardened steel gear pins supported by axial brass bushing.

The HS-7950TH has been designed for the most demanding hobby applications including the largest aircraft and monster trucks. Featuring a titanic 403 oz./in. of torque at 6.0 volts, while still maintaining a respectable 0.15 second transit time.

Features

- G2 Digital Circuit
- Titanium Gear Train (MK first gear)

- Ultra Performance Coreless Motor
- Heatsink Case
- (8) O-Rings for Water/Dust/Fuel protection
- Dual Ball Bearing Supported Output Shaft

Programmable Features Include:

- Dead Band Width
- Direction of Rotation
- Speed of Rotation (slower)
- End Points
- Neutral Points
- Fail Safe On/Off
- Fail Safe Point
- Resolution* (default is high resolution)
- Overload Protection* (default is off)

Specifications

- Motor Type: Coreless
- Bearing Type: Dual Ball Bearing
- Speed (6.0V/7.4V): 0.15 / 0.13
- Torque oz./in. (6.0V/7.4V): 403 / 486
- Torque kg./cm. (6.0V/7.4V): 29.0 / 35.0
- Size in Inches: 1.57 x 0.79 x 1.50
- Size in Millimeters: 39.88 x 20.07 x 38.10
- Weight oz.: 2.40
- Weight g.: 68.04

D.6.5 Receiver [13]

FrSky TFR6M 2.4Ghz 6CH Micro Receiver FASST Compatible



Specification

| | | | |
|-----------|-----------|---------|--------|
| SKU: | 236000003 | Brand: | FrSky |
| Weight(g) | 34.00 | Length | 160.00 |
| Width: | 20.00 | Height: | 87.00 |

D.7 Flight Control Assembly

D.7.1 ESC [9]

Turnigy 20A BRUSHED ESC



Specifications

| | | | |
|-----------|---------|---------|--------|
| SKU: | TGY-20A | Brand: | No |
| Weight(g) | 39.00 | Length | 150.00 |
| Width: | 10.00 | Height: | 110.00 |

D.7.2 GPS Module [11]

UBLOX Micro M8N GPS Compass Module

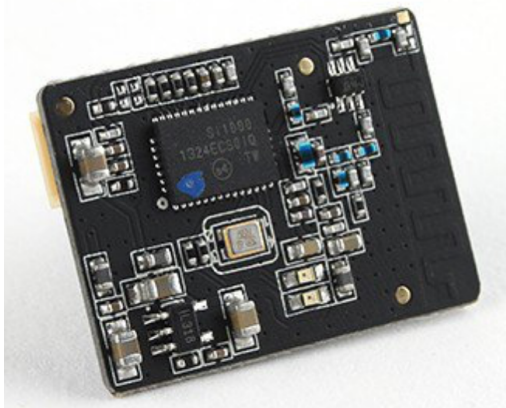


Specifications

| | | | |
|-----------|--------------|---------|-------|
| SKU: | 9387000083-0 | Brand: | No |
| Weight(g) | 29.00 | Length | 80.00 |
| Width: | 10.00 | Height: | 60.00 |

D.7.3 Transceiver [15]

Micro HKPilot Telemetry Radio Set with Integrated PCB
Antenna 915Mhz



Specifications

Supply voltage: **3.7-6 VDC**

Transmit current: **100 mA at 20 dBm**

Receive current: **25 mA**

Serial interface: **3.3 V UART**

Size: **19x25x5mm (with antenna)**

Weight: **1.6g (with antenna)**

Specs Ground Transceiver:

Supply voltage: **3.7-6 VDC (from USB or DF13 connector)**

Transmit current: **100 mA at 20 dBm**

Receive current: **25 mA**

Serial interface: **3.3 V UART**

Size: **25.5x 53x11 mm (without antenna)**

Weight: **11.5g (without antenna)**

| | | | |
|-----------|-------------|---------|--------|
| SKU: | 387000067-0 | Brand: | No |
| Weight(g) | 44.00 | Length | 100.00 |
| Width: | 40.00 | Height: | 70.00 |

D.7.4 Flight Controller [10]

PixFalcon Micro PX4 Autopilot



Specifications

| | | | |
|-----------|--------------|---------|--------|
| SKU: | 9387000082-0 | Brand: | N/A |
| Weight(g) | 99.00 | Length | 107.00 |
| Width: | 40.00 | Height: | 74.00 |

Appendix E: Engineering Drawings

E.1 Parts List

E.2 Complete System Drawing

including cross sections

E.3 Sub-Assembly Drawings

E.4 Individual Part Drawings

Appendix F: Meeting Minutes

F.1 Group Meeting Minutes

| Group Minutes | | | | | |
|---|-------------------------------------|--|---|---|---|
| Attendees: Alex Pennell (apenn095@uottawa.ca,7334789) Isaak Goldenberg (igold093@uottawa.ca,7395188) Joey Kane (jkane035@uottawa.ca,7386330) Sawyer Woodside (swood079@uottawa.ca,7158568) | | Absent: none | Date & Time: 10:30 am 6-Sept-2017 | Venue: CBYB02 | |
| Minute taker: Sawyer Woodside Who is filling out this form? | | | Chairperson: Who is organising the meeting? | Sawyer Woodside | |
| | Task What has to be done? | Action What action is required to get it done? | Who Who is responsible? | Duration How long will it take to complete? | Status Has the task been completed? |
| 1 | Formatting Report | Pick software, organize template | Joey, Isaak | 2 hours | No |
| 2 | Find Images | Write descriptions of the different parts, function, history, etc. | All | Ongoing | No |
| 3 | Filing | Set up a Google drive | Alex | 1 hour | Yes |
| 4 | Meeting and Minutes | Decided chair person and taker are the same. Weekly rotation, setup schedule. | Sawyer | 1 hour | Yes |
| 5 | Messaging | Setup Slack software | Sawyer | 10 minutes | Yes |
| Next meeting Chairperson: Sawyer Woodside | | Minute taker: Sawyer Woodside | Date & Time: 11:30am 8-Sept-2017 | Venue: CBY B02 | |

| Group Minutes | | | | | |
|--|--|---|---|---|---|
| Attendees: Alex Pennell (apenn095@uottawa.ca,7334789) Isaak Goldenberg (igold093@uottawa.ca,7395188) Joey Kane (jkane035@uottawa.ca,7386330) | | Absent: Sawyer Woodside | Date & Time: 08:30 am 13-Sept-2017 | Venue: CBYB02 | |
| Minute taker: Who is filling out this form? Alex Pennell | | Chairperson: Who is organising the meeting? Alex Pennell | | | |
| | Task What has to be done? | Action What action is required to get it done? | Who Who is responsible? | Duration How long will it take to complete? | Status Has the task been completed? |
| 1 | Read through other blimp designs | Use the references in the journal to find other designs | Joey | 4 Hours | In progress |
| 2 | Write section on basic design | Find relevant pictures to use as reference and put in document | Isaak | 6 Hours | In progress |
| 3 | Research attaching the gondola to keel and how it can move | Find relevant picture | Alex | 6 Hours | In progress |
| 4 | Research and summarize regulations | Read through FAA guidelines for airships | Sawyer | 6 Hours | In progress |
| 5 | Write scope and mandate | Start and finish the scope and mandate | Isaak | 2 Hours | Complete |
| Next meeting Chairperson: Alex Pennell | Minute taker: Alex Pennell | | Date & Time: 11:30am 13-Sept-2017 | Venue: CBY B02 | |

| Group Minutes | | | | | |
|---|--|---|---|---|--|
| Attendees: Alex Pennell (apenn095@uottawa.ca,7334789) Isaak Goldenberg (igold093@uottawa.ca,7395188) Joey Kane (jkane035@uottawa.ca,7386330) Sawyer Woodside (swood079@uottawa.ca,7158568) | | Absent: none | Date & Time: 11:30 am 19-Sept-2017 | Venue: DMS | |
| Minute taker: Isaak Goldenberg Who is filling out this form? | | Chairperson: Who is organising the meeting? | Alex Pennell | | |
| Task What has to be done? | Action What action is required to get it done? | Who Who is responsible? | Duration How long will it take to complete? | Status Has the task been completed? | |
| 1 Get rough gondola design ideas | Brainstorm based off of literature review | Alex, Sawyer | 6 Hours | No | |
| 2 Get quote for keel | Put rough 3D out for quotes | Sawyer | 1 Hour | Yes | |
| 3 Get rough dimensions and weights of equipment needed | Find the required components data sheets | Joey, Isaak | 6 Hours | No | |
| 4 | | | | | |
| 5 | | | | | |
| Next meeting Chairperson: Isaak Goldenberg | Minute taker: Isaak Goldenberg | Date & Time: 8:30am 20-Sept-2017 | Venue: CBY C011 | | |

| Group Minutes | | | | | |
|--|---|---|---|---|--|
| Attendees: Isaak Goldenbergberg igold093@uottawa.ca, Joey Kane jkane035@uottawa.ca, Alex Pennel apenn095@uottawa.ca, Sawyer Woodside swood079@uottawa.ca | | Absent: | Date & Time: Sunday, Sept 24th | Venue: Site | |
| Minute taker: Who is filling out this form? | | Chairperson: Who is organising the meeting? | | | |
| Task What has to be done? | Action What action is required to get it done? | Who Who is responsible? | Duration How long will it take to complete? | Status Has the task been completed? | |
| 1 Keel desing, Bearing mounting and Batteries selection | Draw sketches of each design concept, being sketches into overleaf file , explain designs | Isaak | 2 days | | |
| 2 Rack and pinion, position reading, gondola design | Draw sketches of each design concept, being sketches into overleaf file , explain designs | Joey | 2 days | | |
| 3 friction wheel , communication transmission, timing belt, gondola design | Draw sketches of each design concept, being sketches into overleaf file , explain designs | Alex | 2 days | | |
| 4 Mounting thrusters to airship, gondola design, keel desing | Draw sketches of each design concept, being sketches into overleaf file , explain designs | Sawyer | 2 days | | |
| 5 | | | | | |
| Next meeting Chairperson: Joey Kane | Minute taker: Joey Kane | Date & Time: Friday, Sept 29th | Venue: CBY | | |

| Group Minutes | | | | | |
|---|---|---|--|---|--|
| Attendees: Isaak Goldenberg, Igold093@uottawa.ca Joey Kane, JKane035@uottawa.ca Alex Pennell, APenn095@uottawa.ca Sawyer Woodside, SWood079@uottawa.ca | | Absent: None | | Date & Time: Friday, September 29th, 2017 | |
| Minute taker: Who is filling out this form? Sawyer Woodside | | Chairperson: Who is organising the meeting? | | Joey Kane | |
| Task What has to be done? | Action What action is required to get it done? | Who Who is responsible? | Duration How long will it take to complete? | Status Has the task been completed? | |
| 1 Organize and delegate work to all group members | Create an action plan for the modelling report | Joey | 1 Hour | Yes | |
| 2 Demonstrate final design | Draw sketches of each component in detail | Sawyer | 2 Days | No | |
| 3 Compute Gondola Reaction Forces | Create free body diagrams and complete static force analysis on gondola parts | Alex | 3 Days | No | |
| 4 Compute Airship Drag | Create flow simulations in solidworks based on rough dimensions | Joey | 2 Days | No | |
| 5 Find Thrust Values | Review literature to determine best method of calculating thrust | Isaak | 3 Days | No | |
| Next meeting Chairperson: Sawyer Woodside | Minute taker: Sawyer Woodside | Date & Time: Friday, October 6th, 2017 | Venue: CBY | | |

| Group Minutes | | | | | |
|--|--|---|---|--|--|
| Attendees: Isaak Goldenbergberg igold093@uottawa.ca, Joey Kane jkane035@uottawa.ca, Alex Pennel apenn095@uottawa.ca, Sawyer Woodside swood079@uottawa.ca | | Absent: | Date & Time: Friday, October 6th | Venue: CBY | |
| Minute taker: Who is filling out this form? | | Sawyer Woodside | Chairperson: Who is organising the meeting? | Sawyer Woodside | |
| Task What has to be done? | Action What action is required to get it done? | Who Who is responsible? | Duration How long will it take to complete? | Status Has the task been completed? | |
| 1 Gondola Drawings | Draw sketches of each subassembly, how they will be fastened and how they will interact, elaborate in report | Sawyer | 5 days | | |
| 2 Thruster Support Drawings | Draw sketches of each subassembly, how they will be fastened and how they will interact, elaborate in report | Isaak | 5 days | | |
| 3 Wiring and Communications | Specify the design, draw sketches of each design concept (wiring diagrams), elaborate in report | Joey and Alex | 3 days | | |
| 4 Document Tending | Importing Files, formatting, establishing requirements, reworking document template | Alex | 2 days | | |
| 5 | | | | | |
| Next meeting Chairperson: Alex Pennell | Minute taker: Alex Pennell | Date & Time: Friday, October 13th | Venue: CBY | | |

| Group Minutes | | | | | |
|---|---------------------------------|--|---|--|--|
| Attendees: | | Absent: | Date & Time: | Venue: | |
| Isaak Goldenberg igold093@uottawa.ca, Joey Kane jkane035@uottawa.ca, Alex Pennel apenn095@uottawa.ca, Sawyer Woodside swood079@uottawa.ca | | | Thursday, November 2 | CBY | |
| Minute taker: Who is filling out this form? | | Isaak Goldenberg | Chairperson: Who is organising the meeting? | Isaak Goldenberg | |
| | Task What has to be done? | Action What action is required to get it done? | Who Who is responsible? | Duration How long will it take to complete? | Status Has the task been completed? |
| 1 | Solve forces on gondola | Code all equations leaving variables adjustable to solve forces acting on gondola | Isaak | 5 days | |
| 2 | Adjust braking/holding design | Modify braking method in order to not damage and components and ensure efficient braking | All | 5 days | |
| 3 | Organize Sw files | Begin to set up solid works parts for final design | Sawyer | 3 days | |
| 4 | Manufacturing method finalizing | Decide on manufacturing methods for each component | Joey | 2 days | |
| 5 | Set up git hub for coding | | Alex | 5 days | |
| Next meeting Chairperson: Isaak Goldenberg | | Minute taker: Isaak Goldenberg | Date & Time: Thursday, November 2 | Venue: CBY | |

| Group Minutes | | | | | |
|--|--|---|---|---|---|
| Attendees: Isaak Goldenberg, igold093@uottawa.ca Joey Kane, jkane035@uottawa.ca Sawyer Woodside, swood079@uottawa.ca Alexander Pennell, apenn095@uottawa.ca | | Absent: N/A | Date & Time: 8th of November, 2017 | Venue: Isaak Goldenberg's Home | |
| Minute taker: Who is filling out this form? Joey Kane | | Chairperson: Who is organising the meeting? Joey Kane | | | |
| | Task What has to be done? | Action What action is required to get it done? | Who Who is responsible? | Duration How long will it take to complete? | Status Has the task been completed? |
| 1 | Begin design of final solidworks files. | Solidworks parts and assemblies need to be created, equation based | Sawyer | 10 days | No |
| 2 | Begin parametrization | Create matlab directories, input equations from modelling report | Alex, Isaak | 5 days | No |
| 3 | Create LaTeX document | Format document and begin writing section | Joey | 2 days | No |
| 4 | Redo analysis | Redo some section of analysis report, as well as extra analysis as recommended by the TAs | Joey | 3 days | No |
| 5 | | | | | |
| Next meeting Chairperson: Sawyer Woodside | Minute taker: Joey Kane | Date & Time: November 15th, 10am | Venue: CBY | | |

F.2 Team-Partner Meeting Minutes

| Team/Partner Minutes | | | |
|---|------------------------|---|-------------------------------|
| Attendees: Alex Pennell (apenn095@uottawa.ca,7334789) Isaak Goldenberg (igold093@uottawa.ca,7395188) Joey Kane (jkane035@uottawa.ca,7386330) Sawyer Woodside (swood079@uottawa.ca,7158568) | Absent: none | Date & Time: Sept-15-2017 | Venue: C011 and lab |
| Minute taker: Who is filling out this form? | | Chairperson: Who is organising the meeting? Eric Lanteigne | |
| Minutes | | | |
| <p>Discussed overview of the project Wires can cause issues with the system Need to use propellers, since they are more efficient Looked at previous designs Main focus of the project is to design the gondola, other changes to the blimp are extra</p> | | | |
| Next meeting Chairperson: | Minute taker: | Date & Time: | Venue: |

Appendix G: Recommendations for Improving the Course

lol